



**Departamento de Física
da Universidade de Coimbra**

Doppler Flowmetry

Line Imaging Techniques

Project Report
5th year
Graduation in Biomedical Engineering

Edite Maria Areias Figueiras

September 2007





Faculdade de Ciências e Tecnologia
da Universidade de Coimbra



Faculdade de Medicina
da Universidade de Coimbra

This report is made fulfilling the requirements of **Project**, a discipline of the 5th year of the Biomedical Engineering graduation course.



Supervisors	Prof. Carlos M. Correia and Prof. Luís Requicha Ferreira Physics Department FCTUC	
External Supervisor	João Maldonado, MD Instituto de Investigação e Formação Cardiovascular	

Contents

Acknowledgments	i
Abstract	ii
Resumo	iii
Acronyms	iv
1 – Introduction	1
1.1 – Motivation	1
1.2 – Objective	2
1.3 – Outline of this work	2
1.4 – References	3
2 – Theoretical background	4
2.1 – The skin and the blood perfusion	4
2.2 – The Doppler Effect	6
2.3 – Optical Doppler Effect	8
2.4 – The appropriate wavelength	11
2.5 – References	12
3 – State of the Art	13
3.1 – Laser Doppler Flowmetry	13
3.2 – Commercial instruments	16
3.2.1 – PeriScan PIM 3 System	16
3.2.2 – moorLD12	17
3.2.3 – moorLDLS	18
3.2.4 – moorFLPI	19
3.3 – References	20
4 – Components of the system	21
4.1 – Operation principle	21
4.2 – Diagrammatic description	22
4.3 – Optical components	23
4.3.1 – Light source	23

4.3.1.1 – Modulated laser	24
4.3.1.2 – Thin line laser	24
4.3.2 – Line camera	25
4.3.2.1 – 1024 Pixel Line Camera	25
4.3.2.2 – Alternative camera	27
4.4 – Hardware components	28
4.4.1 – Motor	28
4.4.1.1 – Brushless motor	28
4.4.1.2 – Stepper motor	29
4.4.2 – Optical and electromechanical limit switches	31
4.5 – Electronic components	31
4.5.1 – Electronic box	31
4.5.1.1 – NI USB-6008	32
4.6 – Conclusions and future work	33
4.7 – References	34
5 – Software	35
5.1 – System control	35
5.1.1 – Data Acquisition Toolbox	35
5.1.2 – Primitive functions	36
5.1.3 – Combined sequences	36
5.1.3.1 – Dynamic image collection	36
5.1.3.2 – Static image collection	38
5.1.3 – The DAT limitations	39
5.2 – Camera control	39
5.2.1 – Image Acquisition Toolbox	39
5.2.2 – Image acquisition procedure	39
5.2.3 – The IAT limitations	40
5.3 – Frame processing	40
5.4 – Conclusions and future work	40

5.5 – References	41
6 – Results	42
6.1 – Dimensioning	42
6.2 – Hydraulic system	43
6.3 – Functional tests	44
6.4 – Conclusions and future work	47
Annex A – Data Sheet RS Laser	48
Annex B – Data Sheet Thin Line Laser	51
Annex C – Data Sheet 1024 Pixel Line Camera	55
Annex D – Data Sheet Objective	79
Annex E – Data Sheet AVIIVA M2 Line Scan Camera	80
Annex F – Data Sheet Brushless Motor	82
Annex G – Data Sheet NI USB-6008	88

Acknowledgments

This report is the result of the work developed under orientation of Prof. Dr. Carlos M. Correia and Prof. Dr. Luís Requicha Ferreira, of the Physics Department of the University of Coimbra.

This work would not have been possible without the valuable support of some people to whom I would like to express my appreciation.

My most sincere thanks to my supervisors and mentors of this project. Many thanks for all their availability, concern and spent time. Without them this work could not ever been carried through.

Many thanks to Dr. João Maldonado for the idea conceived of this work and his availability in yielding the institute for the accomplishment of tests.

I also would like to thank to Eng Augusto for his help concerning the machining of metallic parts.

I want to thank the elements of the Center of Electronic and Instrumentation, availability and given support.

I want to thank my friends and colleagues for the support and incentive during these last years.

In a special way I want to thank my family and closer friends for the constant moral support and encouragement demonstrated during the good and bad moments I went through during this period.

To all they, my profound thanks for the given help in the elaboration of this work.

Abstract

Laser Doppler Perfusion Imaging (LDPI) has become a standard method for optical measurements of blood perfusion.

This project report describes the design and performance of a bench model of a high-speed LDPI system for monitoring blood flow over a small area of skin tissue.

The system is composed by a line camera, a laser line generator, a brushless motor, a single axis positioning table, two sets of limit switches (optical and electromechanical), a data acquisition module (National Instruments (NI) USB-6008) and an electronic support system (power supplies, interfaces, etc).

These hardware components are completed by two Matlab toolboxes: Image Acquisition Toolbox (IAT), version 2.9, and Data Acquisition Toolbox (DAT), version 1.8 that controls them and does the data acquisition and analysis. The DAT deals with the NI USB-6008 used in three main control functions: the motor, the laser line generator and the reading of the optical limit switches. The IAT is used to control the camera.

Resumo

A imagiologia da perfusão por Laser Doppler tem-se transformado no principal método óptico para a medição da perfusão sanguínea.

Este trabalho descreve o projecto e o desenvolvimento de um modelo de bancada de um sistema de Imagiologia Laser Doppler para a monitorização do fluxo sanguíneo numa pequena porção de pele.

O sistema é composto por um sensor de linha, um gerador de linha laser, um motor sem escovas, uma mesa de posicionamento, dois conjuntos (ópticos e electromecânicos) de interruptores de fim de curso, um módulo de aquisição de dados (National Instruments (NI) USB-6008) e um sistema electrónico de suporte (alimentação, interface, etc).

Estes componentes são controlados por duas toolboxes do Matlab: a Image Acquisition Toolbox (IAT), versão 2.9, e a Data Acquisition Toolbox (DAT), versão 1.8. O DAT permite o controlo da NI USB-6008 que é usada para controlar o funcionamento do motor, do gerador de linha laser e para a leitura dos interruptores ópticos de fim de curso. A IAT é usada para controlar o sensor de linha.

Acronyms

BLDC	Brushless DC Motor
CMBC	Concentration of Moving red Blood Cells
DAT	Data Acquisition Toolbox
DC	Direct Current
FFT	Fast Fourier Transform
fps	Frames per second
GUI	Graphical User Interface
IAT	Image Acquisition Toolbox
LDF	Laser Doppler Flowmetry
LDPI	Laser Doppler Perfusion Imaging
LDPM	Laser Doppler Perfusion Monitoring
NI	National Instruments
Perf	Perfusion
RBC(s)	Red Blood Cell(s)
ROI	Region of Interest
rpm	Revolutions per minute

Introduction

In this chapter, the motivation and objectives of this work will be outlined. A brief summary of the organization of this report will also be made.

1.1 Motivation

Over the last years, the cardiologist community has granted an increasing degree of importance to arterial microcirculation as an indicator of the general hemodynamic condition in humans. In fact, apart from playing a central role in the regulation of the metabolic, hemodynamic and thermal state of the individual ^[1], researchers are now uncovering its correlation with other conditions and diseases. Deepening the knowledge in these areas has, therefore, become a major goal pursued by the medical community.

The majority of flow measurement methods have been developed for use in cardiac flow assessments for the mapping of flow conditions in the major vessels and in the vessels located in the periphery of the vascular tree. The reason for focusing development efforts in this part of the circulatory system is easy to understand. In industrialized countries, approximately 50% of deaths are related to circulatory disorders ^[2].

This fact explains the considerable clinical interest in problems such as arteriosclerosis, obstructive and/or occlusive diseases in the heart, and in the major arteries. The end stages of these diseases are often dramatic and attract a great deal of interest from many researchers with theoretical as well as clinical interests. In spite of the early discoveries of the existence of a microcirculatory network, the methods to study this part of the circulatory system are less developed in comparison with those available for flow measurements in the major vessels. The main reason for this is the complexity of the 3D microcirculation network.

Most flow-measuring probes available today, cause trauma that might seriously disturb the blood flow of microcirculation in the part of the organ into which the probe is introduced. Flow measurement in the microcirculation requires non-invasive procedures or approaches causing little or no trauma. It is also important to find measurement principles that do not disturb the circulation ^[2].

In order to successfully diagnose and treat these diseases, the Laser Doppler Flowmetry (LDF) technique has been the one that has shown the most interesting developments in the clinical perspective and, as a result, it has developed over the years from experimental tools into commercial products^{[3][4]}.

However, the dependence of the LDF signal on the microvascular architecture is not yet well known. Neither in the literature nor in the commercially available instrumentation does a consensus exist about a metric for quantifying blood perfusion. The results presented in the literature are generally expressed in arbitrary units (A.U.), remaining in the open the definition of a quantity that satisfactorily represents what in a theoretical model would be expressed in ml/seg./vol. of tissue (ml per second per volume of tissue). A perfect understanding and knowledge of the LDF signal origin is therefore not yet available for clinicians.

1.2 Objective

The present study aims at developing instrumental methods (prototypes and algorithms) for the assessment of blood perfusion (arterial microcirculation). It describes the design of a LDPI system for monitoring blood flow over an area of tissue using a line imaging technique.

1.3 Outline of this work

This document is organised as follows:

In chapter 2, two separate theoretical overviews are made. The first one focuses the basic physiologic aspects of the main target of the system – the skin. The second outlines the physics of the Doppler Effect and speculates on how it applies in the case of line imaging.

In chapter 3, an outline of the development of the LDF and the current status of some available instruments for assessing blood perfusion is made.

Chapter 4 deals with the basic principle of operation of the system. A description of the bench model and the performance of each of its parts is made.

In chapter 5, all routines for controlling the camera, the laser line generator and the motor, as well as software for analysing the collected data, are explained.

Theoretical background and subsequent values estimations, when applied to this prototype, are developed in chapter 6. The objectives of a specially built hydraulic test system are presented and the functional tests explained.

As a general rule, at the end of each chapter, conclusions are drawn and suggestions for future work or developments are made.

1.4 References

- [1] Stern M. D., “In vivo evaluation of microcirculation by coherent light scattering”, in *Nature*, Vol. 254, March, 1975, pp. 56-58.
- [2] Öberg P. Å., “Optical Sensors in Medical Care”, in *Sensors Update 13*, Sweden, 2004, pp. 201-232.
- [3] Nilsson G. E., Salerud E.G., Strömberg T., and Wårdell K., “Laser Doppler perfusion monitoring and imaging, in *Biomedical Photonics Handbook*”, T. Vo-Dinh, Eds., CRC Press, Boca, Raton, London, New York, Washington DC, 2003.
- [4] Shepherd A. P., and Öberg P. Å., “Laser-Doppler blood flowmetry”, in *Kluwer Academic Publishers*, Boston, Dordrecht, London, 1990

Theoretical background

In this chapter, two separate theoretical overviews will be made. The first one focuses the basic physiologic aspects of the main target of the system – the skin. The second outlines the physics of the Doppler Effect and speculates on how it applies in the case of line imaging.

2.1 The skin and the blood perfusion

The anatomy of the human skin is shown in figure 2.1 and it consists of three layers: the epidermis, dermis and hypodermis.

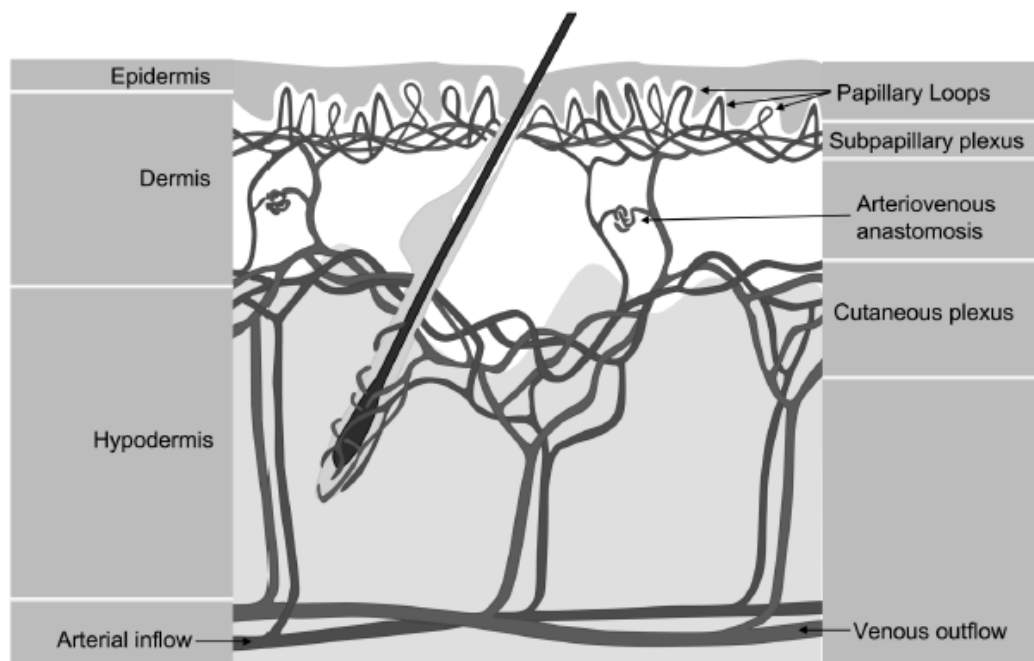


Figure 2.1 A model of the human skin ^[1].

The epidermis is the most superficial layer. It functions as a protecting cover, is avascular, and is quite transparent to light, especially near-infrared radiation.

The dermis is located underneath the epidermis. It contains a microvascular network of arterioles, capillaries and venules that provides the tissue with nutrients and

eliminates waste products. The microvascular network is known as microcirculation (blood perfusion).

The blood perfusion includes the blood flow through vessels smaller than 100 μm , including small arteries (arterioles), capillaries, small veins (venules), and shunting vessels (arteriovenous anastomosis). It comprises the blood vessels of the most peripheral part of the vascular tree ^[1]. The main functions of the microcirculation are transporting blood cells and substances to/from the tissues, and as body coolant in thermoregulation processes. It also contributes to tissues colour and stiffness ^[2].

Microvascular blood perfusion is influenced by time fluctuations and spatial variability. Time fluctuations may be either rhythmic, as in the case of vasomotion, or more stochastic, and have a local or a central origin; spatial variability originates in the anatomical heterogeneity of the microvascular network. Perfusion of blood in the skin is influenced by external factors such as heat, topically applied vasoactive substances and by the intake of beverages and drugs, as well as by smoking or by mental stimuli. In addition, microvascular blood perfusion is regulated via the autonomous nervous system and through vasoactive agents released by the endocrine glands into the bloodstream ^[3].

This blood flow can be altered by diseases like peripheral arterial occlusive disease, diabetes mellitus, allergic reactions, and tumours. In addition, impaired circulation in association with diabetes and peripheral vascular disease may lead to the formation of ulcers and ultimately to tissue necrosis. Consequently, the perfusion of blood in the skin as well as in other tissues needs to be investigated by the use of non-invasive methods with a minimal influence on the parameters under study. Such methods should preferably record the perfusion in real time and be applicable in experimental and clinical settings ^[3].

The dermal microvasculature of dermis consists of a superficial subpapillary plexus and a profound cutaneous plexus (see Figure 2.1). The subpapillary plexus is located at a depth of 400-500 μm from the surface. From the subpapillary plexus, capillary loops (10 μm in diameter) arise toward the *stratum basale* to deliver blood to this active epidermal cell generating tissue, the papillary loops. Therefore, this blood flow is referred to as nutritional flow. The subpapillary plexus is connected by ascending arterioles and descending venules to the cutaneous plexus, located at about 1.9 mm from the surface of the skin. In some areas like fingertips, nose, lips and ears, there are interconnections between these two plexuses often provided with vascular shunts (arteriovenous anastomoses). The shunting vessels are meant to enable a fast increase or decrease of blood

flow through the skin to regulate the body temperature. This thermoregulatory flow prevents the body from large temperature changes ^[1].

The hypodermis is the deepest skin layer and it is not present in body areas where the skin is thin. It functions as a thermal insulation and a mechanical shock protector. Most of the blood flow paths, through this skin layer, are composed by pairs of ascending arterioles and descending venules. Other structures like hair follicles and glands are surrounded by a small capillary network ^[3].

2.2 The Doppler Effect

Christian Doppler first proposed the effect in 1842 in the monograph *Über das farbige Licht der Doppelsterne und einige andere Gestirne des Himmels - Versuch einer das Bradleysche Theorem als integrierenden Theil in sich schliessenden allgemeineren Theorie (On the coloured light of the binary refracted stars and other celestial bodies - Attempt of a more general theory including Bradley's theorem as an integral part)*. The hypothesis was tested for sound waves by the Dutch scientist Christoph Hendrik Diederik Buys Ballot in 1845. He confirmed that the sound's pitch was higher as the sound source approached him, and lower as the sound source receded from him. Hippolyte Fizeau discovered independently the same phenomenon on electromagnetic waves in 1848. It is often overlooked that in Doppler's publications (and also Einstein's in his discussion of the Doppler Effect) he explicitly acknowledges that his formulae are only approximate since he made several mathematical approximations in his derivation ^[4].

The Doppler Effect is the change in frequency of a wave as perceived by an observer moving relative to the source of the waves. For waves that propagate in a medium, such as sound waves, the velocity of the observer and the source are reckoned relative to the medium in which the waves are transmitted. The total Doppler Effect may therefore result from either the motion of the source, or the motion of the observer. Each of these effects is analyzed separately. The waves emitted by the source are either compressed (if the source and detector are moving towards each other) or spread out (if they are moving away from each other). For waves which do not require a medium, such as light or gravity in special relativity, only the relative difference in velocity between the observer and the source needs to be considered ^[4].

For waves that travel through a medium (sound, ultrasound, etc...) the relationship between observed frequency f' and emitted frequency f is given by:

$$f' = \left(\frac{v}{v \pm v_s} \right) f \quad 2.1$$

where v is the speed of waves in the medium and v_s is the velocity of the source ^[4].

The Doppler Effect that occurs with light has a problem because the frequencies of the light waves are very high and difficult to measure directly. This problem is solved by using the phenomenon of ‘beats’ – the effect that is produced when two similar waves of slightly different frequency are superimposed. As the two waves come into and out of phase, they alternately add and cancel. The result is the detection of a frequency that is equal to the difference in frequency between the two waves.

By mixing the Doppler-shifted wave with a reference wave of the original frequency, a beat frequency is produced that is much lower than either of the two constituent waves and is therefore much easier to measure. As this beat frequency is equal to the difference between the two frequencies, it is hence equal exactly to the frequency shift produced by the Doppler Effect ^[5].

It can be shown that the relationship between the frequency change and the relative velocity of the source and the detector is given by

$$f' - f = \frac{v}{c-v} \times f \quad 2.2$$

Where f is the original frequency of the light, f' is the shift frequency, v is the relative velocity of the source and the detector and c is the velocity of the wave. In the case of light waves, the velocity of light c is usually much larger than the velocities being measured and the anterior equation can be simplified to

$$f' - f = \frac{v}{c} f \quad 2.3$$

Hence the frequency shift, and therefore the beat frequency when the Doppler-shifted light is mixed with a reference beam of the original frequency, is proportional to the velocity being measured. All it needs, in addition, is the original frequency and the velocity of light ^[6].

The correct understanding of the Doppler Effect for light requires the use of the Special Theory of Relativity. In this case, however, the relativistic correction of the Doppler Effect is not used because blood moves much slower than light.

To summarize, when light is scattered by a moving object it will be frequency shifted depending on the movement of the object, the direction of the incoming light and the direction of scattered light. When coherent light is scattered from a complex medium

which is in internal motion, the spectral line is broadened by the Doppler Effect in a manner characteristic of the velocity distribution of the motion ^[6].

2.3 Optical Doppler Effect

Coherent light directed toward a tissue will be scattered by moving objects and by static tissue structures as the photons migrated through the tissue in a random pattern. Scattering in moving objects, predominantly red blood cells (RBCs), changes the frequency of the light according to the Doppler principle, while light scattered in static structures alone remains unshifted in frequency. If the remitted light is detected by a photodetector, optical mixing of light shifted and unshifted in frequency will result in a stochastic photocurrent. The power spectral density depends on the number of RBCs and their shape and velocity distribution, within the scattering volume ^[7].

Assume a red blood cell moving with the velocity \mathbf{v} . When light hits the cell, its propagation vector changes from \mathbf{k}_i to \mathbf{k}_s , see figure 2.2.

The angle between \mathbf{k}_i and the projection of \mathbf{v} in the plane of scattering, $\mathbf{v}_{//}$, is denoted by ψ , the scattering angle between \mathbf{k}_i and \mathbf{k}_s is denoted by θ and the angle between \mathbf{v} and $\mathbf{v}_{//}$ is denoted by α . By definition, the scattering vector, \mathbf{q} , is the difference between the propagation vectors for incoming and scattered light, $\mathbf{k}_i - \mathbf{k}_s$ ^[7].

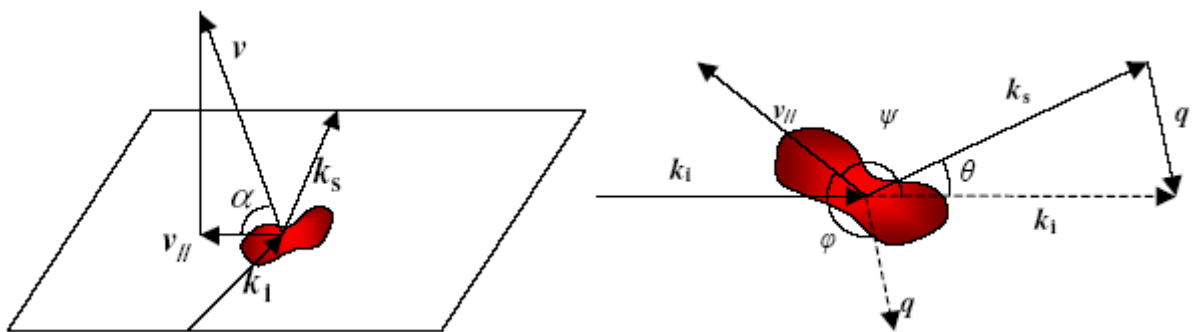


Figure 2.2 Vectorial model of a red blood cell moving and being hit by a light wave ^[7].

The incoming light wave has an angular frequency β_i and a wavelength of $\lambda_i = 2\pi/|\mathbf{k}_i| = 2\pi c/\beta_i$, where c is the speed of light in the tissue. Follow a peak of the wave that is located one wavelength, λ_i , from the cell (at time t_0) and then reaches the cell at time t_1 , as shown in figure 2.3. At this time the cell has moved a small distance ^[7].

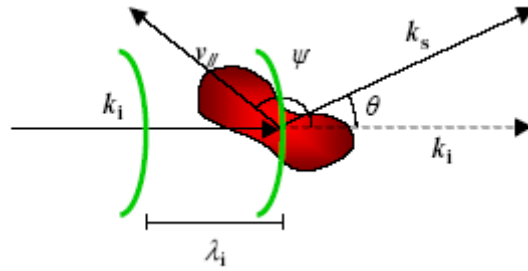


Figure 2.3 A photon with wavelength λ_i hits a red blood cell with velocity v [7].

As $v = |v| \ll c$ the total travelling distance between t_0 and t_1 for the peak can be calculated as

$$\lambda_i + vk_i\lambda_i(t_i - t_0) = \lambda_i + v(t_i - t_0) \cos \psi \cos \alpha = c(t_i - t_0)\alpha \quad 2.4$$

$$(t_i - t_0) = \frac{\lambda_i}{c - v \cos \psi \cos \alpha} \quad [7]. \quad 2.5$$

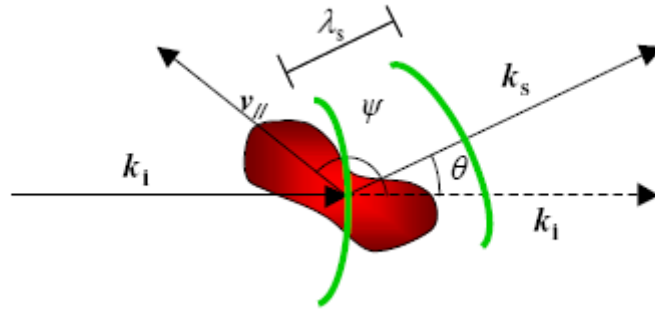


Figure 2.4 After scattering the photon will have the wavelength λ_s [7].

In the meantime the peak that was at the red blood cell at time t_0 has scattered with the angle θ and moved relative the cell, and thus the other peak, a distance (assuming $|v| \ll c$)

$$\lambda_s = c(t_i - t_0) - v(t_i - t_0) \cos(\psi - \theta) \cos \alpha \quad 2.6$$

$$= [\text{Using equation 2.5}]$$

$$= \frac{\lambda_i - \lambda_i \frac{v}{c} \cos(\psi - \theta) \cos \alpha}{1 - \frac{v}{c} \cos \psi \cos \alpha} \quad [7]. \quad 2.7$$

This distance is the wavelength of the scattered light (figure 2.4). The frequency shift, β_D , can now be calculated as the difference between frequency of the scattered light, $\beta_s = 2\pi c/\lambda_s$, and the frequency of the incoming light, $\beta_i = 2\pi c/\lambda_i$:

$$\beta_D = \beta_s - \beta_i = 2\pi \left(\frac{1}{\lambda_s} - \frac{1}{\lambda_i} \right) = \frac{2\pi c}{\lambda_i} \left(\frac{1 - \frac{v}{c} \cos \psi \cos \alpha}{1 - \frac{v}{c} \cos(\psi - \theta) \cos \alpha} - 1 \right) \quad 2.8$$

$$= \frac{2\pi c}{\lambda_i} \left(\frac{1 - \frac{v}{c} \cos \psi \cos \alpha - 1 + \frac{v}{c} \cos(\psi - \theta) \cos \alpha}{1 - \frac{v}{c} \cos(\psi - \theta) \cos \alpha} \right) \quad 2.9$$

$$\approx [\text{Using: } v \ll c]$$

$$\approx \frac{2\pi c}{\lambda_i} (\cos(\psi - \theta) - \cos \psi \cos \alpha) \quad [7]. \quad 2.10$$

It can be seen in equation 2.9 that $\lambda_s \approx \lambda_i$, again since $v \ll c$, and consequently that $|\mathbf{k}_i| \approx |\mathbf{k}_s|$.

The propagation vectors of the incoming and scattered light and their difference, the scattering vector $\mathbf{q} = (\mathbf{k}_i - \mathbf{k}_s)$, thus forms an isosceles triangle with the angles θ and $(\pi - \theta)/2$, see figure 2.5. The angle between \mathbf{k}_i and $\mathbf{v}_{//}$, ψ , can now be calculated as a function of the angle between \mathbf{q} and $\mathbf{v}_{//}$, φ , and the scattering angle between \mathbf{k}_i and \mathbf{k}_s , θ

$$(\psi - \varphi) + \left(\varphi - \frac{\pi - \theta}{2} \right) = \pi \Rightarrow \psi = \frac{\theta}{2} - \varphi + \frac{3\pi}{2} \quad [7]. \quad 2.11$$

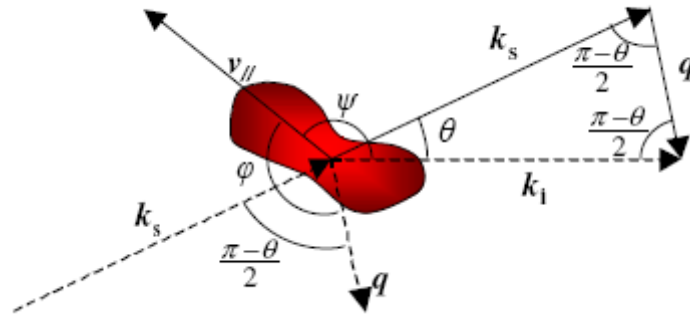


Figure 2.5 Relations between the angles [7].

Using equation 2.11, equation 2.9 can be written

$$\beta_D = \frac{2\pi v}{\lambda_i} \left(\cos \left(\frac{\theta}{2} - \varphi + \frac{3\pi}{2} - \theta \right) - \cos \left(\frac{\theta}{2} - \varphi + \frac{3\pi}{2} \right) \right) \cos \alpha \quad 2.12$$

$$\begin{aligned} &= \frac{2\pi v}{\lambda_i} \left(\sin \left(-\varphi - \frac{\theta}{2} \right) - \sin \left(-\varphi - \frac{\theta}{2} \right) \right) \cos \alpha = \frac{2\pi v}{\lambda_i} 2 \cos \left(\frac{1}{2} (-2\varphi) \right) \sin \left(\frac{1}{2} (-\theta) \right) \cos \alpha \\ &= -\frac{4\pi}{\lambda_i} |\mathbf{v}| \cos \varphi \sin \frac{\theta}{2} \cos \alpha = -\mathbf{q}\mathbf{v} \quad [7]. \quad 2.13 \end{aligned}$$

In capillary blood flow applications, the RBCs velocity is around 10^{-3} m/s. In blood flow studies in the microcirculation the frequency difference is in the order of 10^1 - 10^4 Hz [8].

2.4 The appropriate wavelength

Biological tissues are strongly inhomogeneous from the optical point of view and have a refractive index greater than one. This means that a light beam directed towards a tissue volume is partly reflected at the air-tissue interface and partly penetrates the tissue. Absorption and scattering will broaden the beam and reduce the intensity of the penetration path. In the epidermis, scattering is weak but in the dermis scattering from collagen fibres and cellular organelles is a significant factor in limiting the depth of penetration of radiation [6]. Absorption in the vascular dermis is dominated by the blood-borne pigments such as the haemoglobin contained in the RBCs [9]. Absorbed light is converted into heat or will be re-radiated as fluorescent radiation [6].

Absorption spectra are strongly dependent on tissue composition and especially on water content. At ultraviolet and infrared wavelength most of the light is absorbed in water and an incident beam only penetrates a few cell diameters into the tissue. Visible light with shorter wavelengths (green, yellow) penetrates 0.5-2.5 mm and undergoes an exponential decay in intensity. Both scattering and absorption occur in this spectral region. In the near IR and IR parts of the spectrum scattering is the most pronounced optical phenomenon to consider. In these parts of the spectrum, photons penetrate approximately 10 mm into the tissue [8].

The transmitted light undergoes scattering in the tissue in a very complicated way. Light is refracted in the microscopic inhomogeneities, formed by cell membranes, collagen fibers, and sub-cellular structures. Pigments such as oxyhemoglobin, and bilirubin absorb the diffuse light. Anderson and Parrish have given the wavelength-dependent absorption characteristics of these pigments [10]. In human skin, the spectral range 600-1600 nm has very good penetration for light. This part of the spectrum is often called the therapeutic window because it makes deeper tissue layers accessible [8].

2.5 References

- [1] Morales F., “Improving the clinical applicability of laser Doppler perfusion monitoring”, M.S. thesis, Groningen Univ., November, 2005.
- [2] <http://en.wikipedia.org/wiki/Microcirculation>
- [3] Nilsson G. E., Salerud E. G., Strömberg N. O. T., Wårdell K., “Laser Doppler Perfusion Monitoring and Imaging”, In: Vo-Dinh T, editor. Biomedical photonics handbook, Boca Raton, Florida: CRC Press; 2003. p. 15:1-24.
- [4] http://en.wikipedia.org/wiki/Doppler_effect
- [5] Briers J. D., “Laser Doppler, speckle and related techniques for blood perfusion mapping and imaging”, Physiological Measurement, Institute of Physics Publishing, October, 2001, pp. R35-R62
- [6] Stern M. D., “In vivo evaluation of microcirculation by coherent light scattering”, in Nature, Vol. 254, March, 1975, pp. 56-58.
- [7] Fredriksson I, Fors C and Johansson J, “Laser Doppler Flowmetry – a Theoretical Framework”, Department of Biomedical Engineering, Linköping University, 2007.
- [8] Öberg P. Å., “Optical Sensors in Medical Care”, in Sensors Update 13, Sweden, 2004, pp. 201-232.
- [9] Jones D P, “Medical Electro-Optics: Measurements in the Human Microcirculation”, Physic Technology 18, 1987.
- [10] Anderson R R and Parrish J A, “Optical Properties of Human Skin”, in The Science of Photomedicine. Plenum Press, New York, 1987, pp. 147-194.

State of the art

In this chapter, an outline of the development of the LDF and the current status of some available instruments for assessing blood perfusion will be made.

3.1 Laser Doppler Flowmetry

Thanks to the invention of the laser in the early 1960s by Hecht, a number of optical investigative and therapeutic tools are now available in physiology laboratories or in the clinical environment. Amongst these one of the most representatives is LDF ^[1].

LDF is a continuous and non-invasive method for tissue blood flow perfusion, utilizing the Doppler shift of a low powered laser light as the information carrier. By illuminating a tissue sample with single-frequency light and processing the frequency distribution of the backscattered light an estimate of blood perfusion can be achieved ^[2].

The first measurements of microvascular blood flow employing the Doppler shift of monochromatic light were made on retinal blood flow of a rabbit in 1972 ^[3]. Some years later the blood velocity of exposed microvessels was investigated by use of a laser Doppler microscope. In vivo evaluation of skin microcirculation by the use of coherent light scattering was first demonstrated by M. D. Stern in 1975. In this setup, in which a He-Ne laser beam illuminates the skin, a portion of the laser is scattered by moving blood cells as well as static tissue structures, while the remaining light is scattered by static tissue structures alone. If the backscattered Doppler-broadened light is brought to the surface of a photodetector, the speckle pattern appearing on the detector surface fluctuates because of the optical mixing of waves of different frequencies. These fluctuations are manifested as audiofrequency components in the photocurrent superimposed on a steady baseline. Analysis of the photocurrent reveals a clear shift of the spectral content toward lower frequencies following the occlusion of the brachial artery by use of a pressure cuff placed around the upper arm and with the laser beam aimed at the fingertip. This fundamental discovery was soon implemented in a portable fibber-optic-based laser Doppler flowmeter,

which provided results comparable with those obtained by the Xe-clearance technique for assessment of tissue blood perfusion ^[4].

As LDF based equipments were commercialized in the early 1980s, Laser Doppler Perfusion Monitoring (LDPM) became available to a wide range of researchers and clinicians. The ease of use of this new technology quickly created an extensive interest in recording microvascular perfusion in a wide variety of disciplines ^[4].

One of the most remarkable features of microvascular blood perfusion is its substantial time and space variability. Consequently, the comparatively small sampling volume (about 1 mm³) of fiber-optic-based LDPM instruments constitutes one of the main limitations of this technology: with the spatial variability in tissue blood perfusion gross differences in perfusion readings may appear at recordings from adjacent sites. This disadvantage of LDPM triggered the development of multichannel instruments and the LDPI technology at the end of the 1980s. In LDPI, an airborne laser beam scans the tissue and successively records the tissue perfusion from a number of sites with no need for physical contact with the tissue. From these data a two-dimensional colour-coded perfusion map of the microvascular perfusion is generated. It has reported the use of LDPI in the connection of tissue perfusion of the skin, intestinal mucous, and cutaneous malignancies ^{[5][6]}. The commercialization phase of the LDPI-technology started in the early 1990s, and several hundred publications have already verified its usefulness, particularly in dermatology, wound healing, and burn treatment ^[4].

The theory which is used to compute, from the raw LDF signals, the blood flow and/or speed related parameters appears to be fundamentally the same for LDPM and LDPI ^[7].

The Concentration of Moving red Blood Cells (*CMBC*) and the perfusion (*Perf*) can be estimated from the Doppler power spectrum $P(\omega)$. These estimates are not absolute measures but, in a given sample with low RBC concentration, *CMBC* and *Perf* scale varies linearly with the RBC concentration and the tissue perfusion, respectively. In LDF, perfusion is defined as the RBC concentration times the average RBC speed. Thus,

$$CMBC \propto C_{RBC} \quad 3.1$$

$$Perf \propto C_{RBC} \langle v_{RBC} \rangle \quad 3.2$$

where C_{RBC} is the RBC concentration and $\langle v_{RBC} \rangle$ the average RBC speed. For high concentrations of RBCs the *CMBC* and *Perf* estimates varies nonlinearly with C_{RBC} , while the relationship between perfusion and the average RBC velocity is entirely linear,

provided that C_{RBC} is constant and the frequency distribution of the photocurrent is within the bandwidth of the system, as shown in figure 3.1.

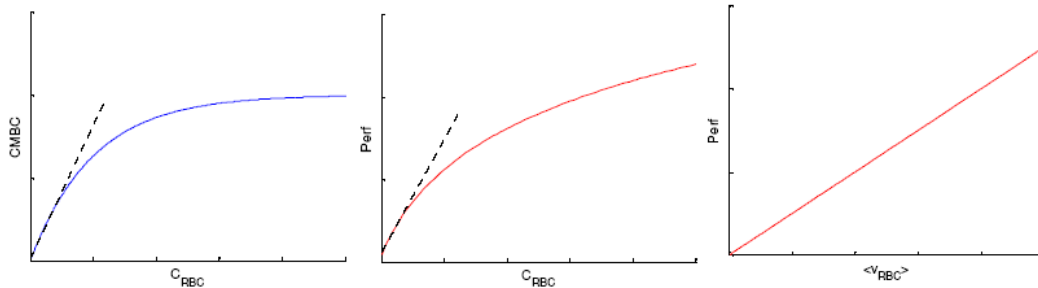


Figure 3.1 Approximate relationships for CMBC and CRBC (left), Perf and CRBC (middle) and Perf and $\langle v_{RBC} \rangle$ (right), when all other variables are kept constant ^[2].

The *CMBC* is proportional to the integral of the Doppler power spectrum and can be written in the form

$$CMBC \propto \int_0^{\infty} P(w)dw \quad [2]. \quad 3.3$$

The perfusion is proportional to the integral of the frequency-weighted Doppler power spectrum and can be written in the form

$$Perf \propto \int_0^{\infty} wP(w)dw \quad [2]. \quad 3.4$$

It is frequently assumed that RBCs represent the majority of the blood-borne objects in the undisturbed microcirculation, but this technique does not selectively record the movement of RBCs.

Currently, LDF does not give an absolute measure of blood perfusion. In the clinical setting this is a limiting factor and the reason why LDF instruments are not routinely used in health care. However, LDF has found its use in research. Among the applications are pharmacological trials, allergy patch testing, wound healing, physiological assessments and skin disease research ^[4]. The skin is probably the most LDF studied organ but also internal organs such as kidneys, liver, muscles, intestines, brain and heart have been investigated in a number of studies ^[2].

Several commercial instruments are available today, some of which present colour-coded images of microcirculatory flow patterns, giving spatial and time information ^[8].

3.2 Commercial instruments

3.2.1 PeriScan PIM 3 System

The PeriScan PIM 3 System, in figure 3.2, is a LDPI system for non-invasive imaging of superficial tissue blood perfusion.



Figure 3.2 PriScan Pim 3 ^[9].

It is operated from a standard PC and the patented scanning technique offers excellent image integrity, sensitivity and perfusion baseline stability. The technique can be used to monitor microcirculatory activity in healthy and diseased tissue, and show basal values and also responses resulting from an applied physiological stimulus, a provocation. An example of a result obtained as showed in figure 3.3 ^[9].

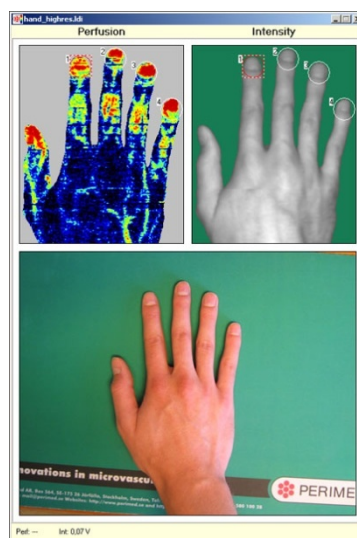


Figure 3.3 Results of Periscan Pim 3 ^[9].

3.2.2 moorLDI2

The moorLDI2 laser Doppler, presented in figure 3.4, images the tissue surface and maps blood flow. A full resolution scan includes 65,536 individual laser Doppler measurements and these are displayed alongside a corresponding 'photo' image, as a colour coded image ^[10].



Figure 3.4 moorLDI2 ^[10].

The moorLDI2 laser Doppler blood perfusion imagers use a near infra-red laser beam (785nm in the standard moorLDI2-IR imager) or a visible red 633nm laser beam (moorLDI2-VR imager). In the moorLDI2-2 λ dual wavelength system 633 and 830nm lasers are combined to allow simultaneous imaging with the two wavelengths. An example of a result obtained as showed in figure 3.5 ^[10].

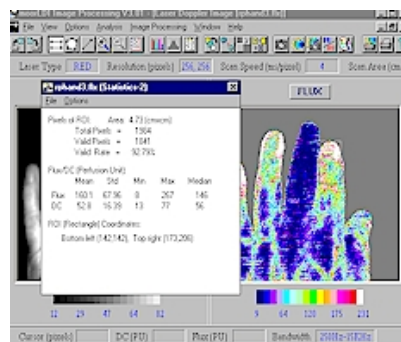


Figure 3.5 Results of moorLDI2 ^[10].

3.2.3 moorLDLS

The moorLDLS (figure 3.6) rapid line scanning system provides laser Doppler images of blood flow in the microvasculature. The system employs a multi channel laser Doppler line to sweep across the tissue gathering data from 64 points simultaneously^[11].



Figure 3.6 moorLDLS^[11].

The system is ideally suited to any application where the dynamic changes are too rapid to be captured by conventional laser Doppler imaging^[11].

3.2.4 moorFLPI

The moorFLPI, showed in figure 3.7, full field blood perfusion imaging system provides video frame rate images of blood flow in the microvasculature up to 25 images per second.



Figure 3.7 moorFLPI ^[12].

Compared to standard laser Doppler imaging the effective sampling depth is small. The resulting image is mainly of blood flow in the microvessels in the surface layers of the tissue being sampled, for example the nutritional flow in skin. In exposed tissue where blood vessels are close to the surface e.g. open surgery, these will also be imaged ^[12].

3.3 References

- [1] Briers J. D., “Laser Doppler, speckle and related techniques for blood perfusion mapping and imaging”, *Physiological Measurement*, October, 2001, pp. R35-R62
- [2] Fredriksson I, Fors C and Johansson J, “Laser Doppler Flowmetry – a Theoretical Framework”, Department of Biomedical Engineering, Linköping University, 2007.
- [3] Riva C, Ross B and Benedek G B, “Laser Doppler measurements of blood flow in capillary tubes and retinal arteries” *Invest. Ophthalmol.* 11, 1972, pp. 936–44.
- [4] Nilsson G. E., Salerud E. G., Strömberg N. O. T., Wårdell K., “Laser Doppler Perfusion Monitoring and Imaging”, In: Vo-Dinh T, editor. *Biomedical photonics handbook*. Boca Raton, Florida: CRC Press; 2003. p. 15:1-24.
- [5] Wardell K., Jakobsson A., Nilsson G. E., “Laser Doppler perfusion imaging by dynamic light scattering”, *IEEE Trans Biomed Eng* 1993, pp. 40:309-316.
- [6] Svanberg K., Andersson T., Killander D., Wang I., Stenram U, Andersson-Engels S, et al, “Photodynamic therapy of non-melanoma malignant tumors of the skin using topical δ -amino levulinic acid sensitization and laser irradiation”, *Br J Dermatol*, 1994, pp. 130:743-751.
- [7] Binzoni T., Leung T. S., Seghier M. L., and Delpy D. T., “Translational and Brownian motion in laser-Doppler flowmetry of large tissue volumes”, *Phys. Med. Biol.* **49**, 2004, pp. 5445–5458.
- [8] Öberg P. Å., “Optical Sensors in Medical Care”, in *Sensors Update 13*, Sweden, 2004, pp. 201-232.
- [9] http://www.perimed.se/p_Products/pim3.asp
- [10] <http://www.moor.co.uk/products/burnassessment/moorldi2>
- [11] <http://www.moor.co.uk/products/imaging/moorldls>
- [12] <http://www.moor.co.uk/products/imaging/moorflpi>

Components of the system

In this chapter, the basic operation principle of the system will be introduced (4.1). A description of the bench model (4.2) and the performance of each of its parts will be made.

The restrictions of some of the used components will be presented and suggestions, for overcoming these limitations, will also be made.

4.1 Operation principle

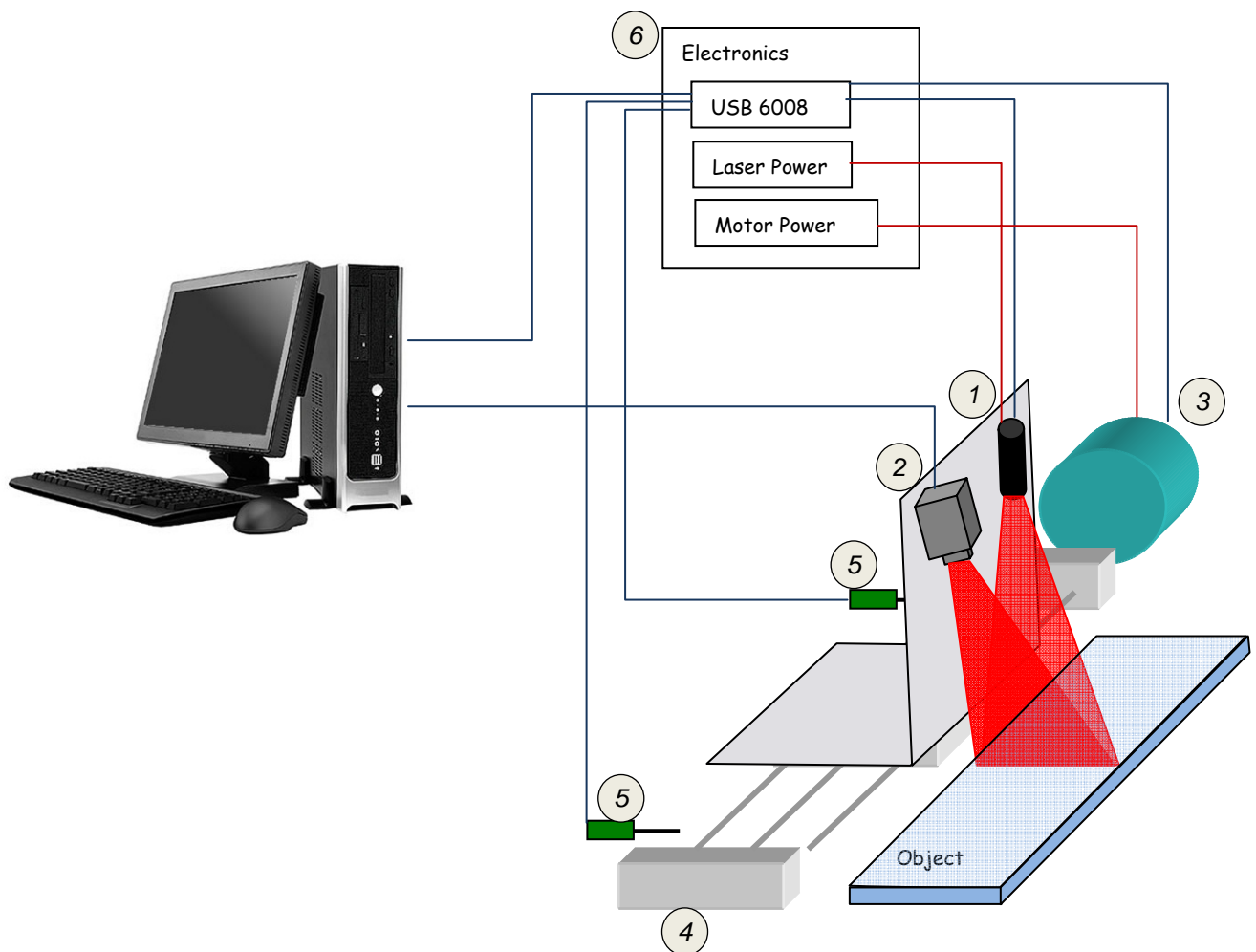


Figure 4.1 Diagrammatic model (1- Laser line generator, 2 – Line camera, 3 – Motor, 4 – Positioning Table, 5- Optical Limit Switches, 6 – Electronic System).

In this type of imager, depicted as a schematic model in figure 4.1, a moving carriage, attached to a positioning table and driven by a suitable motor, holds the illumination laser and the camera while the scanning movement develops. The low power laser beam successively scans the tissue where the laser light is scattered and changes wavelength when it hits moving blood cells (Doppler shift) as was explained in chapter 2. A fraction of the incident light is backscattered and detected by the line sensor. This light forms an interference pattern on the line sensor and the fluctuations in this pattern carry information about the Doppler shifts. The images are acquired line by line, as the illuminating laser line scans the object. Data is recorded by dedicated routines written using Matlab's DAT and IAT.

The moving mechanism is protected from overflow by limit switches placed at both extremes of the course. A double arrangement of electromechanical and optical limit switches was implemented at each extreme. The electromechanical limit switches being there for safety reason: if the software readable optical limit switches fail for some unexpected reason, the electromechanical limit switches act like a hard circuit breaker that cuts power preventing catastrophic movements to occur. The optical limit switches act like limiting indicators, and change the rotation direction of the driving motor.

4.2 Diagrammatic description

The device is a bench model, showed in figure 4.2, mounted in an optical breadboard with threaded holes with metallic parts that were machined at the Physics Department mechanical workshop.

It consists of a laser line generator, a line sensor, a motor, a position table, the limit switches and an electronic system. The electronic system is formed by the NI USB-6008, the electronic system for the optical limit switches and the power supply for the laser (-12V) and the motor (24V). The NI USB-6008 purpose is to control the motor, the laser and to read the output of the optical limit switches. The heavy metallic breadboard permits noise reduction that can occur due to vibrations. The motor is fixed in the breadboard and it is mechanically connected to the position table. It is used to make the scanning movement of the camera and the laser (both mounted in a moving carriage).

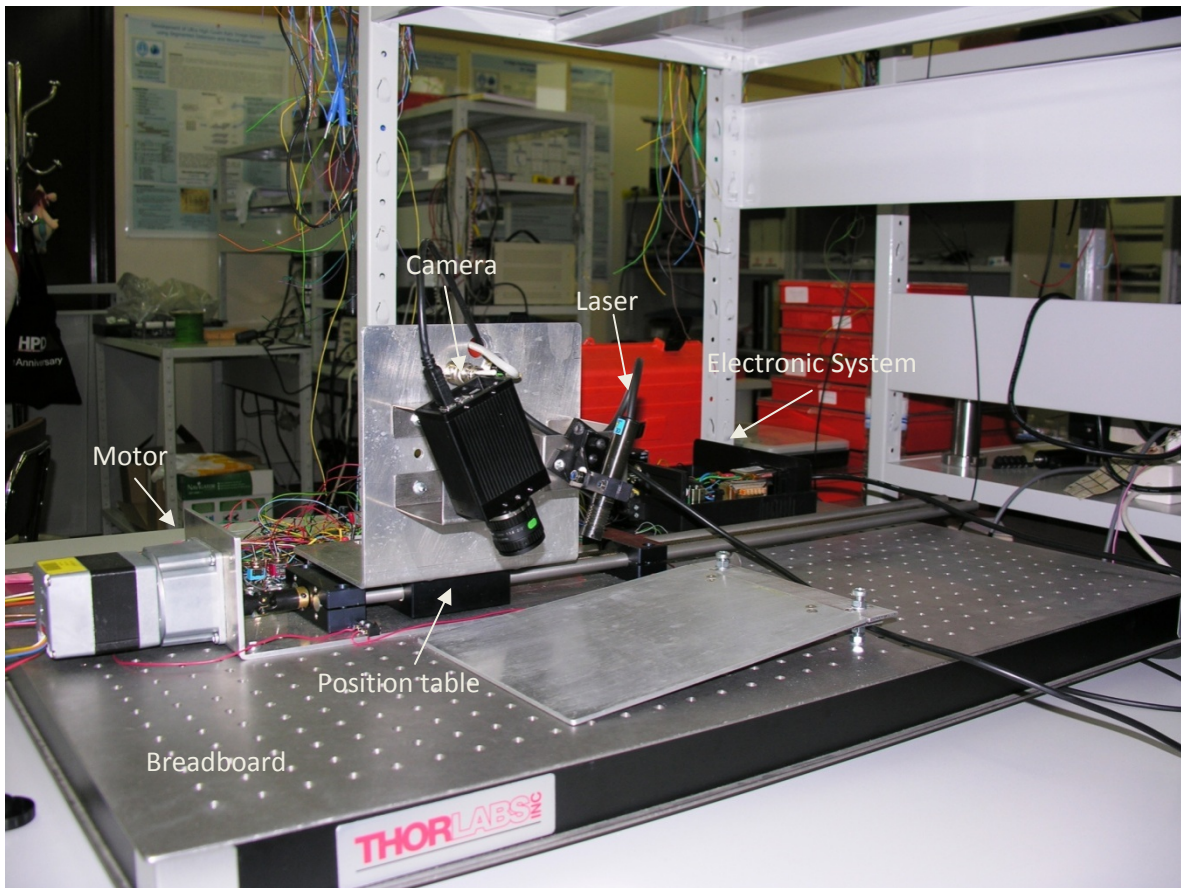


Figure 4.2 Bench model.

4.3 Optical components

4.3.1 Light source

As predicted by the theory, the frequency shifts caused by Doppler scattering will result in a frequency broadening of the originally monochromatic light. Two laser line generators were used in this work. Initially, a modulated laser was acquired, but its line width proved to be too large for this work as well as too difficult to regulate. A very high-quality thin line laser was then acquired for better image resolution.

4.3.1.1 Modulated laser

The modulated laser, showed in figure 4.3, consists of a laser diode, a line generator lens and a driver circuit housed in the metal case.

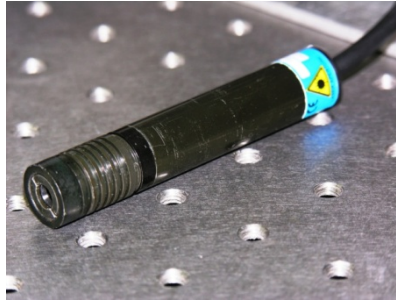


Figure 4.3 Modulated Laser.

The length of the line produced by the line generator is dependent on the focal length of the cylindrical lens while the thickness is dependent on the size of the focussed spot produced by the spherical lens. The greater the operating distance, the larger and thicker is the line.

In practice, the laser line is very thick and hard to deal with.

The wavelength of the modulated laser is 670 nm and the range of the operating voltage is -8 to -12 V.

The modulation capability of this proved to be very useful as it will be explained later (cap 6).

For further information see the general characteristics in annex A.

4.3.1.2 Thin line laser

The thin line laser is a 5 mw, 673.5 nm unit, with 64 mm working distance (figure 4.4). The geometric parameters specified in the data sheet were found to be very convenient: at the working distance the line length is 17 mm and the thickness is 30 μm .



Figure 4.4 Thin Line Laser.

This laser produces even intensity thin lines which predict that the collected data will be more accurate and precise. The superior optical design yields a large depth of field and minimizes variations in thickness across the length of the generated line ^[3].

For further information see the general characteristics in annex B.

4.3.2 Line camera

The line camera purpose is used to collect line frames at a rate high enough to see the frequency beatings associated to the Doppler shifts. Initially, a 1024 pixel unit capable of 10 kfps (frames per second), from ISG, seemed to fulfil the needs of the application. However, experimental work revealed a number of inadequacies that suggest a different unit for the task.

4.3.2.1 1024 Pixel Line Camera

The LightWise LW-ELIS-1024A Line Scan Camera presented in figure 4.5 was used in this work. This 1024 pixel unit is capable of capturing up to 10K lines per second. It provides 16MB on-board image buffering and interfaces via a Standard FireWire™ (1394a) protocol that complies with the IEEE-1394 IIDC DCAM Specification, Version 1.3.



Figure 4.5 1024 Pixel Line Camera.

For further information about the camera see the general characteristics in annex C.

The objective has a focal length of 12 mm and its characteristics are presented in annex D.

In this work the frames were acquired with the ISG Graphical User Interface (GUI) or the IAT. Each frame can be constituted by a maximum of 1024 pixels and 640 lines.

According to the sampling theorem, the maxim beating frequency that the camera is capable of detecting equals half the number of frames per second (fps). This rate is computed as inverse of the sum of the read time with the integration time. To maximize that frequency, the clock frequency (read frequency) was set to 15MHz and the total integration time to 68 μ s. As an example, when an acquisition of frames with 144 pixels/line and 64 lines the frame rate is:

$$\frac{64 \times 144}{15 \times 10^6} + 68,4 \times 10^{-6} \times 64 \approx 200 \text{fps}.$$

So, the maximum frequency of each line is acquired is:

$$200 \text{fps} \times 64 \times 0.5 = 6400 \text{Hz}.$$

With frames with 256 pixels and 64 lines and the same total integration time the maxim frequency is 5849.6 Hz and with frames with 100 pixels and 64 lines the maximum frequency is 6660.7 Hz.

It was used 64 lines because this is considered as minimum number of lines necessary to apply the Fast Fourier Transform (FFT). The number of pixels is much less than 1024 to maximize the frequency that the camera detects, and are adequate to perform the experiments.

The maximum frequency seen by this camera does not comprise the frequency difference produced by microcirculation (10^1 - 10^4 Hz).

4.3.2.2 Alternative camera

The line camera used is not able to see frequency shifts high enough as those produced by the blood velocity. So it was proposed the AVIIVA M2 Line Scan Camera showed in figure 4.6.



Figure 4.6 AVIIVA M2 Line Scan Camera.

The AVIIVA M2 Line Scan Camera is a high-speed and high performance 12 bit output camera with data rates of 60 mega pixels per second (settings available for 8 or 10 bit output).

This camera is proposed because, with a resolution of 512 pixels, the maximum line rate is 109 kHz which is much higher than the previews camera. With this line rate the maximum frequency shift that can be observed is 54.5 kHz which is sufficient for this project, as we can see in calculations shown in chapter 6.

The camera includes a LVDS interface or CameraLink® interface, built-in anti-blooming exposure control functions, no lag effect sensor technology, multi-camera synchronization, flat-field correction and contrast expansion.

The system designer can utilize numerous programmable settings to implement several camera configurations: integration time, gain, offset, trigger mode, calibration (FFC and contrast expansion), and output format ^[5].

For further information cf. the data sheet in annex E.

4.4 Hardware components

4.4.1 Motor

This work has been carried out using a brushless DC motor to drive the positioning table for the scanning movement of the moving carriage. In this section a proposal for a stepper motor is made.

4.4.1.1 Brushless motor

A brushless DC motor (BLDC) was selected to avoid the oscillations associated to the brushes of standard DC motors and, at the same time, retains their capability of delivering a rotation speed proportional to the supply voltage .

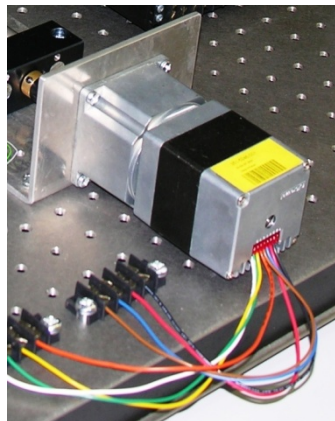


Figure 4.7 Brushless motor.

In a BLDC motor, the electromagnets do not move; instead, the permanent magnets rotate and the armature remains static. This gets around the problem of how to transfer current to a moving armature. In order to do this, the brush-system/commutator assembly is replaced by an intelligent electronic controller. The controller performs the same power distribution found in a brushed DC motor, but using a solid-state circuit rather than an electromechanical commutator/brush system.

BLDC motors offer several advantages over brushed DC motors, including higher efficiency and reliability, reduced noise, longer lifetime (no brush erosion), elimination of ionizing sparks from the commutator, and overall reduction of electromagnetic

interference. The enhanced efficiency is mostly due to the absence of friction of brushes, and it is greatest in the no-load and low-load region of the motor's performance curve. Under high mechanical loads, BLDC motors and high-quality brushed motors are comparable in efficiency. The maximum power that can be applied to a BLDC motor is exceptionally high, limited almost exclusively by heat, which can damage the magnets. BLDC's main disadvantage is higher cost, which arises from two issues. First, BLDC motors require complex electronic speed controllers to run. Second, many practical uses have not been well developed in the commercial sector ^[2].

The major advantage of this brushless motor, showed in figure 4.7, is the fact that the electronic control system is built in, making it easier to use and avoiding any risk for the components. The speed can vary from 10 to 100% by means of a 0-10 V analogue signal or PWM signal (control signal, converted by the electronics to set the speed). The nominal speed ranges from 3410 to 5400 rpm. Two digital inputs are provided respectively for the on-off and rotation direction controls. An encoder output is also available ^[6].

General control of the motor can be switched between manual and automatic. The manual system is based in switches and its purpose is to control the motor if the automatic system failed. The automatic system is made through the NI USB-6008 by routines written using Matlab DAT.

For further information cf. the data sheet in annex F.

4.4.1.2 Stepper motor

Throughout the project it became obvious that when a frame of lines is acquired at a given position, the moving carriage should stand still. Then it should move by a constant amount to take the next frame and repeat this sequence until the entire object is scanned.

A stepper motor is the right choice for this job since it delivers precise, repeatable angular increments that are used to drive the spindle of the positioning table.

A stepper motor is a brushless, synchronous electric motor that can divide a full rotation into a large number of angular steps. Thus the motor can be rotated to a precise angle.

It is an electromechanical device which converts electrical pulses into discrete mechanical angular movements. The shaft or spindle of a stepper motor rotates in discrete step increments when electrical command pulses are applied to it in the proper sequence. The motor's rotation has several direct relationships to these applied input pulses. The

sequence of the applied pulses is directly related to the direction of the motor shaft rotation. The speed of the motor shaft rotation is directly related to the frequency of the input pulses and the angle of rotation is directly related to the number of input pulses applied.

Stepper motors operate differently from normal DC motors, which simply spin when voltage is applied to their power terminals. Stepper motors, on the other hand, effectively have multiple "toothed" electromagnets arranged around a central metal gear (figures 4.8 and 4.9). To make the motor shaft turn, first one electromagnet is fed with current, which makes the gear's teeth magnetically attracted to the fixed electromagnet's teeth. When the gear's teeth are thus aligned to the first electromagnet, they are slightly offset from the next electromagnet. Consequently, when the next electromagnet is turned on and the first is turned off, the gear rotates slightly to align with the next one, and from them on the process is repeated. Each one of those slight angle rotation is called a "step." In that way, the motor can be turned to a precise angle ^[4].

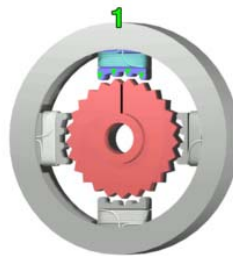


Figure 4.8 The top electromagnet (1) is fed, attracting the topmost four teeth of a sprocket ^[4].

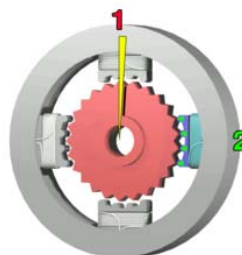


Figure 4.9 The top electromagnet (1) is turned off, and the right electromagnet (2) is fed, pulling the nearest four teeth to the right ^[4].

The stepper has several advantages for this project when compared to the brushless motor. The rotation angle of the motor is proportional to the input number of pulses and

precise positioning and repeatability of movement can be achieved. This fact permits a better control of the covered distance by the motor.

4.4.2 Optical and electromechanical limit switches

The optical and electromechanical limit switches, showed in figure 4.10 and 4.11 respectively, are place at the beginning and at the end of the course and their main purpose is to stop the motor when the moving carriage reaches either of these extremes.

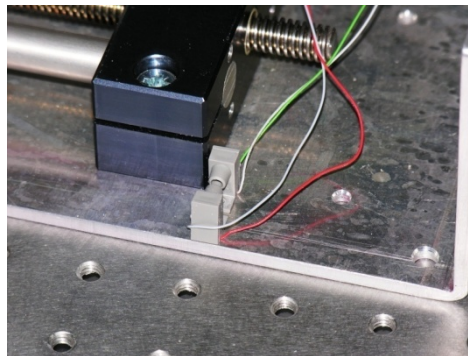


Figure 4.10 Optical limit switches.

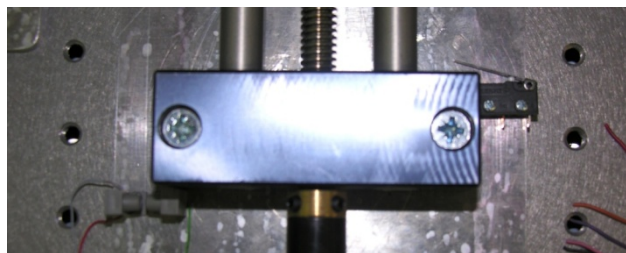


Figure 4.11 Electromechanical limit switches.

The electromechanical limit switch is an emergency system. If the optical limit switch fails the electromechanical system stops the motor.

4.5 Electronic components

4.5.1 Electronic box

The electronic system, shown in fig. 4.12, includes the NI 6008 and the power supplies for the laser (-12V) and for the motor (24V).

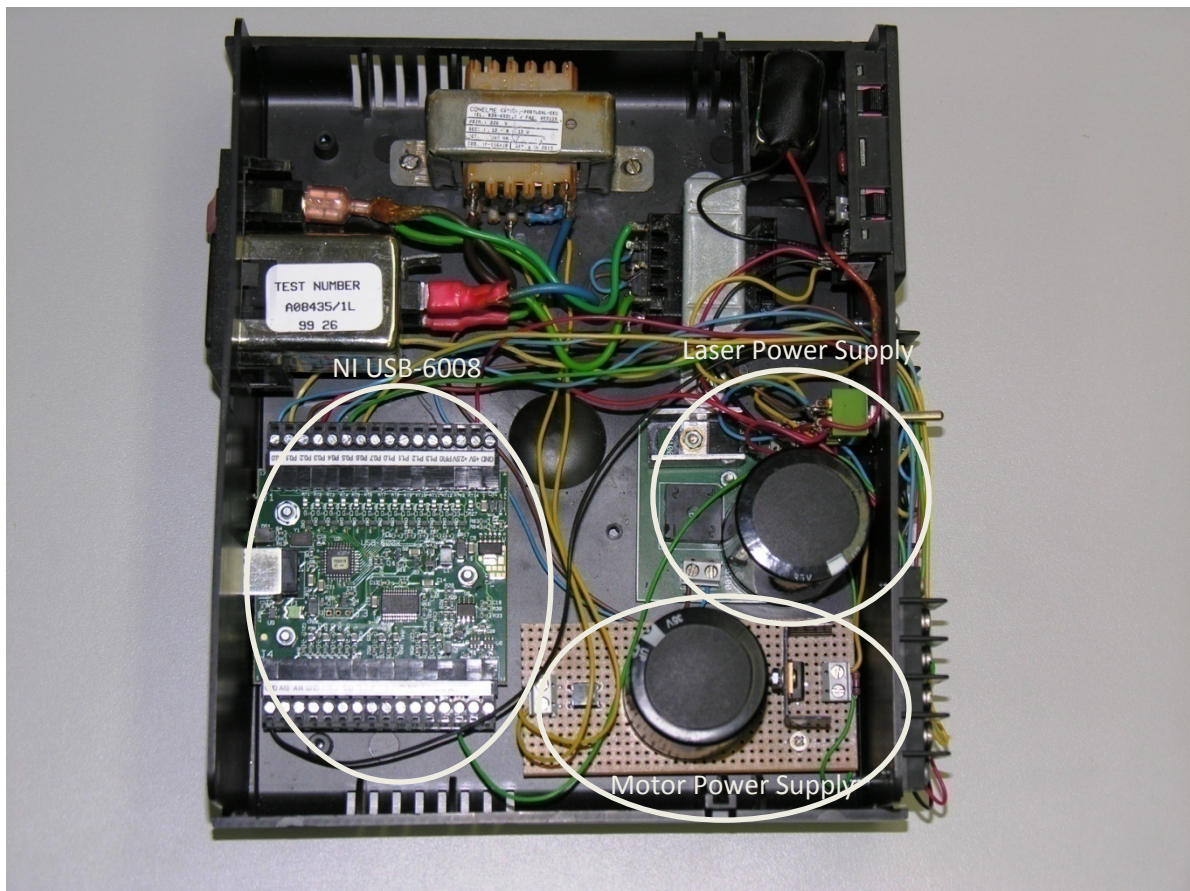


Figure 4.12 Electronic System.

4.5.1.1 National Instrument USB-6008

The NI USB-6008, presented in figure 4.13, is a multifunction data acquisition module. It has a plug-and-play USB connectivity.



Figure 4.13 NI USB-6008.

The NI USB-6008 use the NI-DAQmx high-performance, multithreaded driver software for interactive configuration and data acquisition on Windows.

The NI-DAQmx Base permits to develop customized data acquisition applications with the National Instruments LabVIEW or C-based development environments, like MatLab.

The NI USB-6008 provides connection to eight analogue input channels, two analogue output channels, twelve digital input/output channels, and a 32-bit counter with a full-speed USB interface (an even counter input).

The NI USB-6008 is programmable with MatLab, through DAT. In this work it is used to control the velocity and the direction of the motor, to switch on/off the motor and the laser. It also reads the optical limit switches to detect the ends of course of the moving carriage and it should be able to read the speed of the motor because it has a counter input. However, there is no implementation in the DAT to use the counter.

For further information cf. the data sheet in annex G.

4.6 Conclusions and future work

The thin line laser showed more efficiency than the modulated laser, because the line thickness and the output power that is provide enhances the accuracy and the precision of the collected data.

The line rate of the AVIIVA M2 Line Scan Camera is 54,5kHz which is much superior to the previews camera and it complies with the frequency difference produced by blood flow (10^1 - 10^4 Hz), so this camera is a better choice for a future work.

It is clear that the scanning movement should be advantageously made by a stepping motor because it allows a better control of the covered linear distance, by the motor.

4.7 References

- [1] Fredriksson I, Fors C and Johansson J, "*Laser Doppler Flowmetry – a Theoretical Framework*", Department of Biomedical Engineering, Linköping University, 2007.
- [2] http://en.wikipedia.org/wiki/Brushless_DC_electric_motor
- [3] <http://www.adept.net.au/lighting/lasers/mfl.shtml>
- [4] http://en.wikipedia.org/wiki/Stepper_motor
- [5] http://www.hilltech.com/products/electro_optics/linescan_cameras.html
- [6] <http://www.crouzet-usa.com/articles/bldc.shtml>

Software

In this chapter, a description of the programs that control the NI USB-6008 (5.1) and the line camera (5.2) using the DAT and IAT, respectively, as well as the programmes to process the acquired frames (5.3), will be made.

The limitations of the software packages used will be explained and suggestions for future work will also be drawn.

5.1 System control

5.1.1 Data Acquisition Toolbox

The NI USB-6008 is controlled by the DAT.

Specifically, the DAT supports National Instruments data acquisition hardware that uses the NI-DAQmx driver software. Cf. the table in *i)* for a complete list of supported hardware and the minimum toolbox version required ^[1].

DAT supports three device objects: analogue input, analogue output, and digital I/O.

This work needs one analogue output object, three digital output objects and two digital input objects.

Analogue output functions allow sending signals out to the NI USB-6008. It creates an analogue output object, add one channel, and generate analogue signals to control the motor's rotation velocity.

Digital I/O functions enable to generate or read digital signals using the NI USB-6008. It creates digital I/O objects, add lines, send data to the hardware, and read data into the workspace. Digital output functions are used to turn on and off the motor or the laser, or to change motor's rotation direction. Digital input functions are used to read the optical limit switches.

i) <http://www.mathworks.com/products/daq/supportedio14005.html>

5.1.2 Primitive functions

In first place we describe a function that initializes the NI USB-6008 (Initialization) where the required channels are created: three digital output objects (that control the state of the laser, the motor and the motor's rotation direction); two digital input objects (that read the optical limit switches) and one analogue output object (that control the motor's rotation velocity), was produced.

Then, basic functions that read the output of the optical limit switches, turn on/off the motor and the laser, change the motor's rotation direction and control the motor's rotation velocity, are created. These functions also allow knowing the state of the motor and of the laser (on or off) and the rotation direction (retrieve or advance).

5.1.3 Combined sequences

5.1.3.1 Dynamic image collection

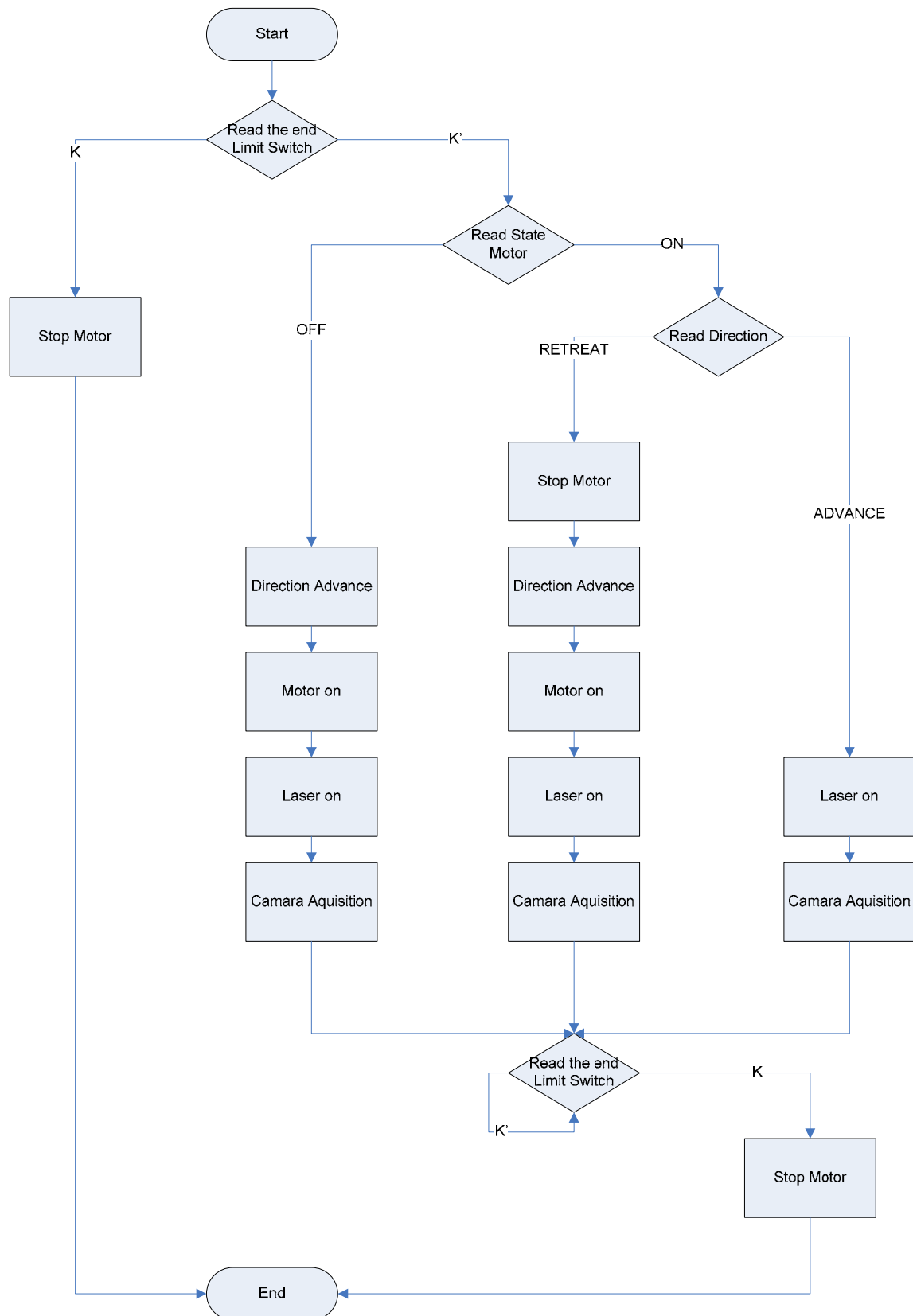
At this stage the images were acquired during the movement of the motor, i.e., the moving carriage does not stop when the camera makes the acquisition.

Two functions were written: one that positions the moving carriage in the beginning of the course (Beginning_Course) and the other that makes the scanning movement (Scanning_Movement).

For the scanning movement, Flowchart 5.1, the function starts by reading the end course optical limit switch. If the moving carriage is already at the end of the course the programme ends. If not, the programme reads the state of the motor. If the motor is stopped, the programme gives the motor advance order, laser on and the camera to acquire using the IAT. If the motor is already moving the programme read the direction of rotation. If the direction is "retreat" the programme stops the motor, changes the direction to "advance", turns on the motor and the laser, and the camera begins to acquire with the IAT. If the direction is already "advance" the function turns on the laser, and the camera begins to acquire with the IAT. After that, in a cycle command, the function reads the end of course optical limit switch, and, when the moving carriage reaches it, the motor stops.

The function "Beginning_Course" has only some differences, when compared to the previews described function. It reads the star_up limit switches, but does not turn on laser and does not order the camera to acquire.

In a completed acquisition programme these functions shall be sequentially implemented.

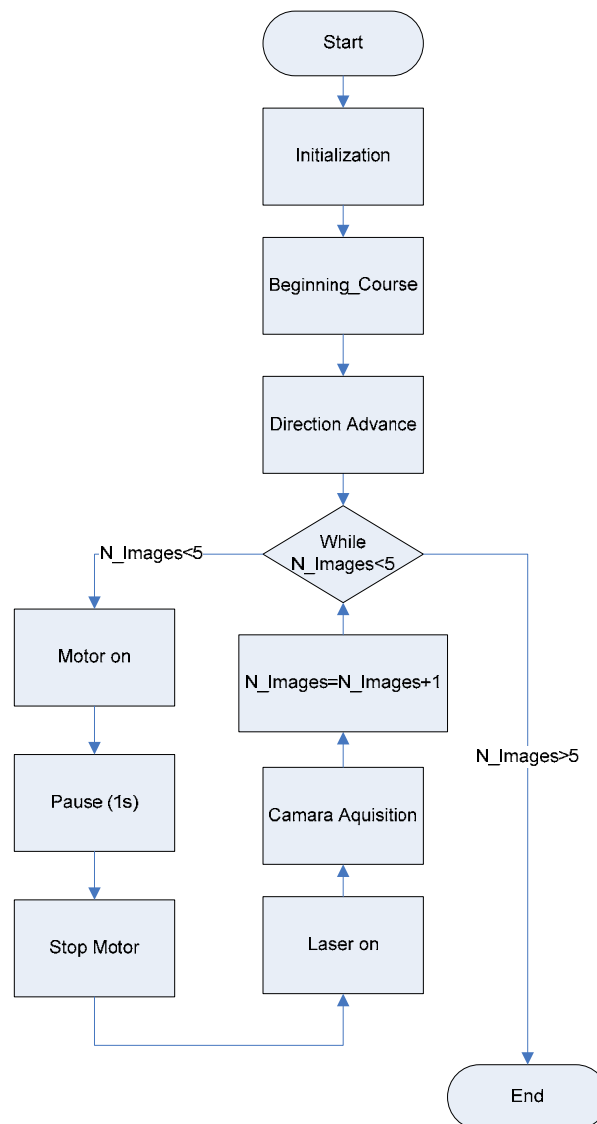


Flowchart 5.1 Programming the scanning movement (K: the moving carriage is in the end of the course; K': the moving carriage isn't in the end of the course).

5.1.3.2 Static image collection

Another program was drawn because it was found as necessary to do the acquisition with the camera standing still. This had to be done in order to have several by lines at same region, for later FFT application.

This programme, represented in flowchart 5.2, uses some of the functions previously created. Firstly it initializes the NI USB-6008, driving the moving carriage to the beginning of the course and implements the direction to “advance”. Then, in a cycle command, it turns on the motor, leaves it running during one minute, stops the motor, turns on the laser and the camera, and does the acquisition of one frame. This cycle is repeated as many times as needed (5 times in the flowchart 5.2).



Flowchart 5.2 Program to acquired frames with the camera stopped. In this example there were acquired 5 frames.

5.1.4 The DAT limitations

The NI USB-6008, as mentioned in 4.6.1, allows configuring a dedicated pin connection as an event counter input, that when connected to the encoder logic output (pulses per revolution) of the motor should allow us to know the covered distance of the moving carriage. However, this function is not yet implemented, which represents a severe drawback still present in ver.2.9 of the DAT.

5.2 Camera control

5.2.1 Image Acquisition Toolbox

The IAT provides functions for acquiring still images and video directly into MATLAB and into Simulink from the PC-compatible imaging hardware.

The toolbox allows to configuring the hardware by modifying the properties of the object associated with it. The properties can be browses and configured using the MATLAB command line or the graphical Property Inspector tool ^[2].

5.2.2 Image acquisition procedure

To use the IAT to acquire imaging data with the 1024 Pixel Line Camera, firstly it is necessary to retrieve information that identifies the camera. Then, a video input object has to be created. After the video input is created it is essential to see a preview of the video stream. If the images are not satisfactory, the characteristics of the image or other aspects of the acquisition process must be modified. The IAT allows several parameter, to be controlled, and set-up and operation of the 1024 Pixel Line Camera. Base properties that can be controlled are: resolution, gain, auto exposure, region of interest (ROI), brightness, shutter, shutter absolute and returned colour space. Finally after setting-up the IAT, the image data can be acquired and logged to the disk.

5.2.3 The IAT limitations

The IAT does not permit full parameter control of the 1024 Pixel Line Camera. An important parameter for this work, like clock frequency, cannot be controlled by the IAT. So, the frames have to be acquired with ISG GUI.

5.3 Frame processing

Processing the frames consists in the application of the FFT at each frame.

FFT is a method for computing the discrete Fourier transform with reduced execution time.

The lines of each frame are images of the same scanned region acquired in successive time intervals. To process these frames, the FFT is applied at each pixel of the frame along the lines that constitute the frame. A 3-D plot is made to see the FFT of all the pixels.

5.4 Conclusions and future work

In the acquisition of the perfusion images it is very important to know the location where the images were collected. So the event counter input of NI USB-6008 would be a crucial channel for this work, since it allows us to know the covered distance by the moving carriage. Unfortunately this channel is not operational in this version of the DAT and it may be necessary, in the future, to use an analogue input of the NI USB-6008 to deal with the encoder output of the motor.

The IAT does not allow full parameter control, so the access to the 1024 Pixel Line Camera has to be made in future via direct access to the module's register set through a lower level programming language.

5.5 References

- [1] <http://www.mathworks.com/products/daq/index.html>
- [2] <http://www.mathworks.com/products/imaq/index.html>

$$f = \frac{4\pi}{670 \times 10^{-9}} \times \sin\left(\frac{135}{2}\right) \times 1 \times 10^{-3} \times \cos(120) \cos(0)$$

$$= 8.664 \text{ KHz.}$$

As calculated in chapter 4, 4.4.1, the maximum frame rate of the camera, tested at the very beginning, is 6660 Hz. This frequency allows the detection of velocities up to $7.69 \times 10^{-4} \text{ m s}^{-1}$.

However, the frequency difference that the camera should be able to detect, as computed in 2.3, is within the range 10^1 - 10^4 Hz.

In conclusion, this camera doesn't allow the system to comply with the sampling theorem criteria.

Another practical difficulty derives from the complexity in realising hydraulic systems with flow velocities lower than 1 mm s^{-1} .

6.2 Hydraulic system

The hydraulic system purpose is to establish a well known flow regime in order to put the system to test.

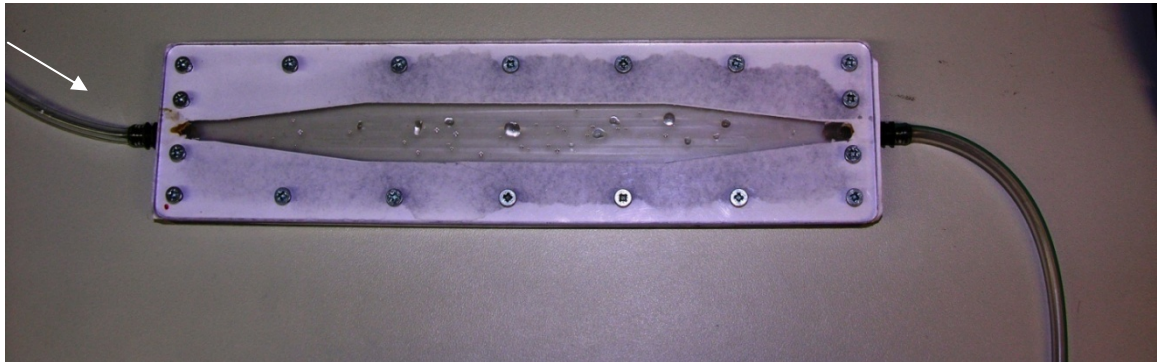


Figure 6.2 Hydraulic System

Photograph of figure 4.14 shows one simple solution for this question. The liquid is a blend of water with talcum powder, which is a good light scatterer, that enters the apparatus by the left side (white arrow) with a certain velocity and evolves to lower velocities with laminar profile, and then again to the initial velocity. Transparent acrylic machined has been used for optical reasons and also for mechanical convenience. This device has a plan central region with known volume where the laminar regime can be

theoretically predicted. This system is gravity driven and the range of estimated velocities is 10^{-3} to 10^{-2} m s⁻¹.

The 1024 Pixel Line Camera does not allow all the range of estimated velocities for this hydraulic system, because the maximum velocity detected by the camera, as calculated in 6.1, is .

6.3 Functional tests

To confirm the calibration of the time axis of the 1024 Pixel Line Camera experiments have been carried out with the modulated laser and a white paper strip used as scatterer. The laser was modulated with different frequencies: 100 Hz, 150 Hz, 200 Hz, 250 Hz, 500 Hz and 1 kHz. In figures 6.2 to 6.4 frames obtained for the modulate frequencies of 100 Hz, 500 Hz and 1 kHz can be seen.



Figure 6.3 Frame obtained for the modulating frequency of 100 Hz.



Figure 6.4 Frame obtained for the modulating frequency of 500 Hz.



Figure 6.5 Frame obtained for the modulating frequency of 1 kHz.

Then the FFT was applied and the results are shown in figures 6.5 to 6.7. As can be seen in the three graphs below, a centred peak occurs at the value of the modulation frequency.

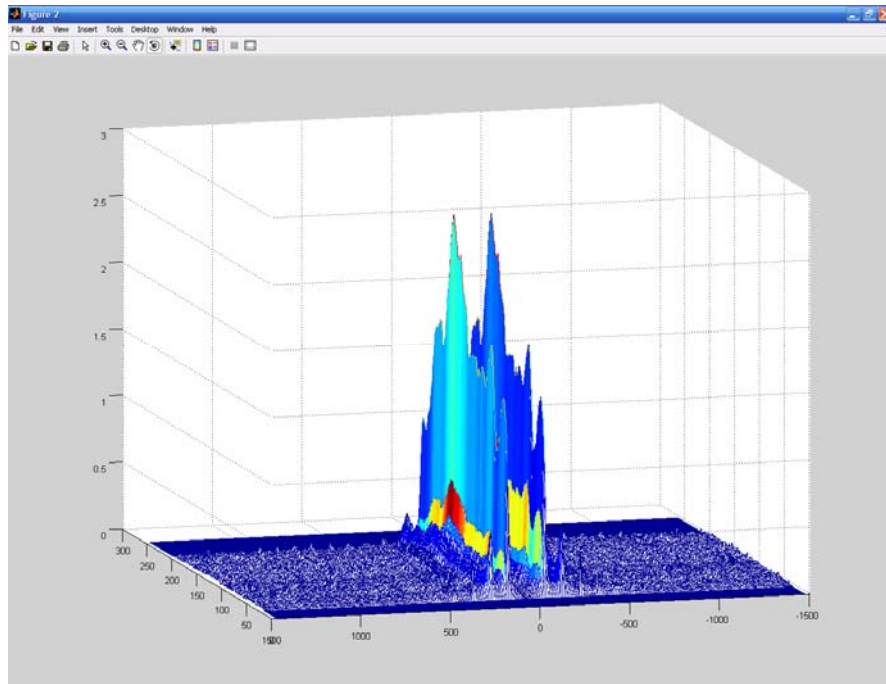


Figure 6.6 Application of FFT to the frame shown in figure 6.2.

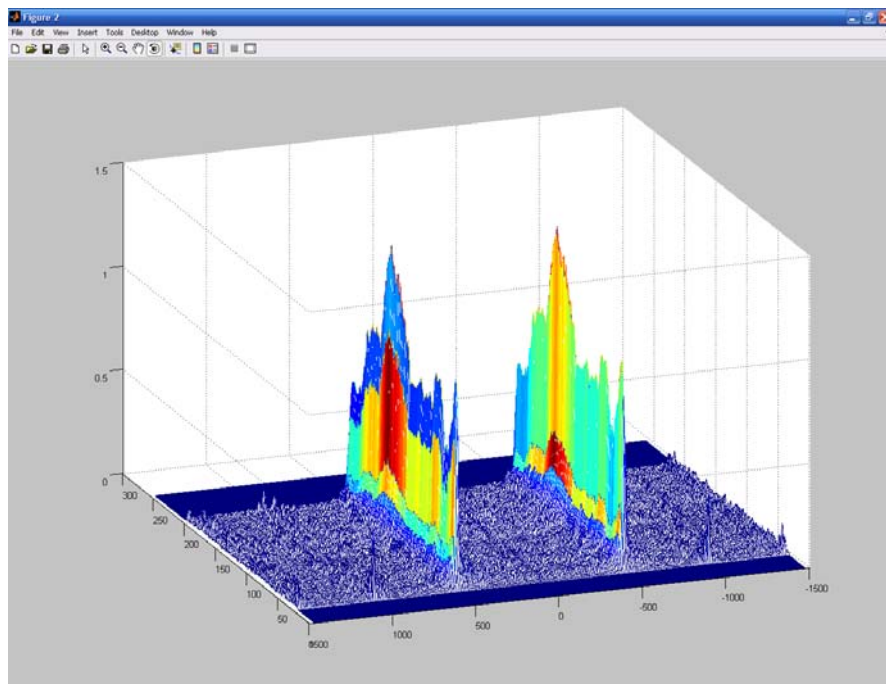


Figure 6.7 Application of FFT to the frame shown in figure 6.3.

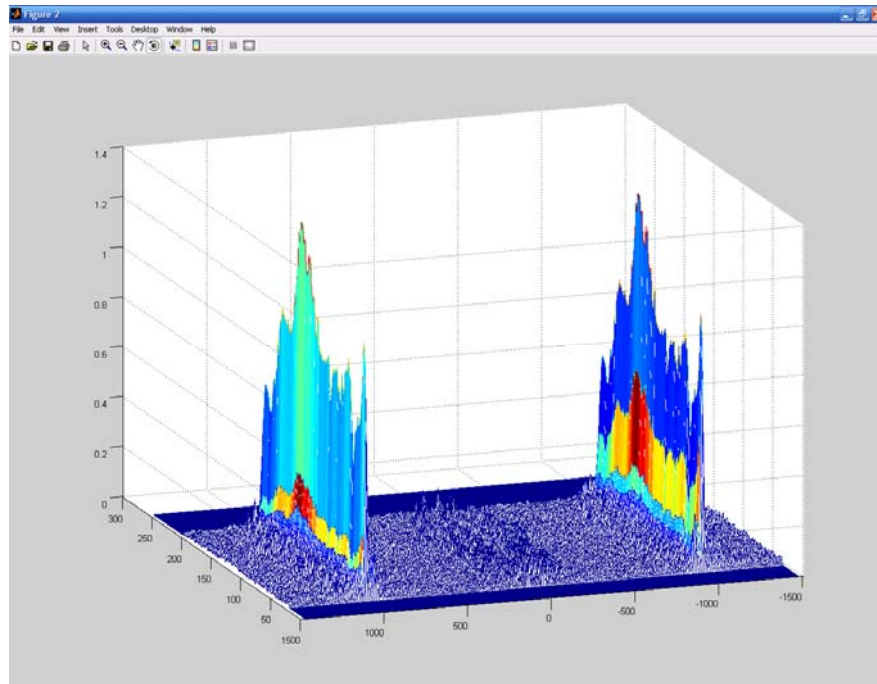


Figure 6.8 Application of FFT to the frame shown in figure 6.4.

We can conclude that for this order of magnitude of the modulation frequency the system performs a correct detection.

6.4 Conclusions and future work

Despite the proved accuracy of the system, the order of magnitude of frequencies in the microcirculation application lays beyond the measurement range of the system. This is mainly due to the line camera limitations. Again, the AVIIVA M2 Line Scan Camera referred in 4.6 is one possible solution to this problem.

This is the reason why there were no results with the hydraulic system unless much lower flow velocities could be established.



Data Sheet

Laser diode modules

This data sheet covers the following items:

Device	RS stock no.
Beta TX series	
1mW modulating	564-504
3mW modulating	194-004
3mW modulating	111-368
Beta CW series	
1mW continuous wave	194-010
1.5mW continuous wave	111-346
3mW continuous wave	111-352
3mW continuous wave	194-026
3mW line generator	194-032
3mW Wide angle line generator	213-3613
Single standard lens	194-048
Line generator lens	194-054
Line generator lens wide angle	213-3629
Laser diode holder	213-3641

Device	RS stock no.
Beta Cameo Series	
0.8mW continuous wave	213-3590
1mW continuous wave	213-3562
3mW continuous wave	213-3584
3mW continuous wave	213-3607

Description

These laser modules consist of a laser diode, lens and driver circuit housed in a metal case. The module body is electrically isolated. Electrical connections are made via flying leads. The lens is a single element of high refractive index glass which produces a high quality collimated beam over a long distance. Its position can be adjusted to bring the beam to a focused spot using the special key provided. The Beta CW and TX series standard collimating lens may be replaced by a line generating lens which produces a fan shaped beam that can be focused to a fine, straight line. (RS stock no. 194-032) is supplied with a line generator lens producing a beam angle of 16° fitted, (RS stock no. 213-3613) is supplied with a line generator lens producing a beam angle of 106° fitted. The lens on the Beta Cameo series cannot be replaced with a line generating lens.

Introduction

These devices have been designed as complete laser diode systems for original equipment manufacturer (O.E.M.) use and although their output powers have been set in accordance with BS(EN)60825, they are not certified lasers as defined in the specification. When incorporated in a piece of equipment it may be necessary for additional safety features to be added before equipment complies fully with the standard. Read BS(EN)60825 before using any of these products.

Continuous wave lasers Beta CW series

General characteristics

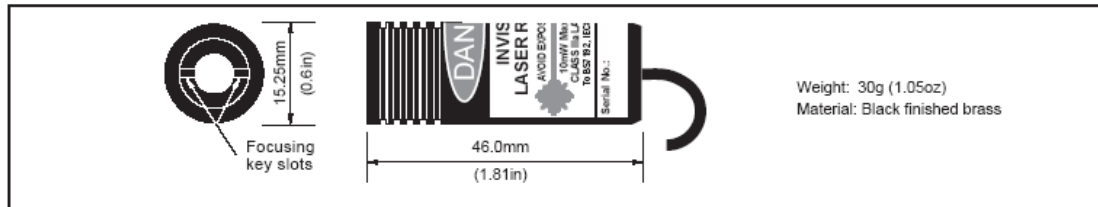
Parameter	RS stock no./Value				Units
	111-346	194-010	194-026 213-3613	111-352	
Nominal wavelength	635	670	670	785	nm
Maximum power output	1.5	1	3	3	mW
Typical power output stability (@ 20°C)	2				%
Typical power output temperature dependence	15				µW/°C
Operating voltage	+4.5 to +5.5	-8 to -12			Volts
Typical operating current at minimum voltage	30 - 75	25 - 45		50 - 80	mA
Typical operating current at maximum voltage	30 - 75	25 - 50		50 - 85	mA
Power supply rejection ratio (50Hz-100kHz)	1.0	0.6			%/V
TTL disable voltage	-	>4			Volts
Maximum TTL pulse rate	-	10			Hz
Mean time to failure (MTTF) @ 30°C	4,500	80,000	20,000	32,000	Hours
Connections	250mm flying leads				
Red lead	+ve supply	-			
Black lead	-	-ve supply			
Green lead	0	0			Volts
Blue lead	-	TTL disable			

Optical characteristics

Parameter	RS stock no./Value				Units
	111-346	194-010	194-028 213-3613	194-032 111-352	
Beam size	4.5 x 2.5	3.5 x 2.5	4.5 x 2.5 100° Fan	4.5 x 2.5	mm
Minimum focus (lens extended)		25		25	mm
Spot size at minimum focus		>50		>50	Micron
Polarisation ratio	90:1	80:1	100:1	60:1	
Pointing stability		<0.05			mRad
Output aperture	6.0	3.5	6.0		mm
Angular deviation of beam to case (front cell)		<5			mRad

The spot size is determined by optical measurement. The relationship of the spot size to illumination is $(\frac{1}{fV})^2$ therefore the size to the human eye will appear bigger.

Mechanical details



Absolute maximum ratings

Parameter	RS stock no./Value	
	111-346	194-010 194-028 111-352 194-032 213-3613
Supply voltage	+6.0V	-12.7V
TTL disable input voltage	-	-3 to +7V
Operating temperature	-10 to +30°C	-10 to +40°C
Storage temperature	-40 to +85°C	

Power supplies and earthing

Laser modules which operate from a negative voltage can be run from an unregulated supply within the range of -8 to -12V. By operating at the lower (-8V) end of the power supply range, less heat will be dissipated within the device and hence the expected life will increase.

Laser modules which operate from a positive voltage may only be run from a supply which has been regulated to at least 5%, within the limits specified.

For all laser modules the case is isolated from the supply voltages.

It is advisable for any floating power supplies to have the '0' volts connection (and if used, the heatsink) taken to ground. If this is not done, then in electrically noisy environments, the power supply leads can act as aerials. Under these conditions any noise picked up can damage the laser module. If a heatsink is not used, then the barrel of the laser module should be grounded.

TTL disable

This feature is only available on laser modules which operate from a negative supply voltage.

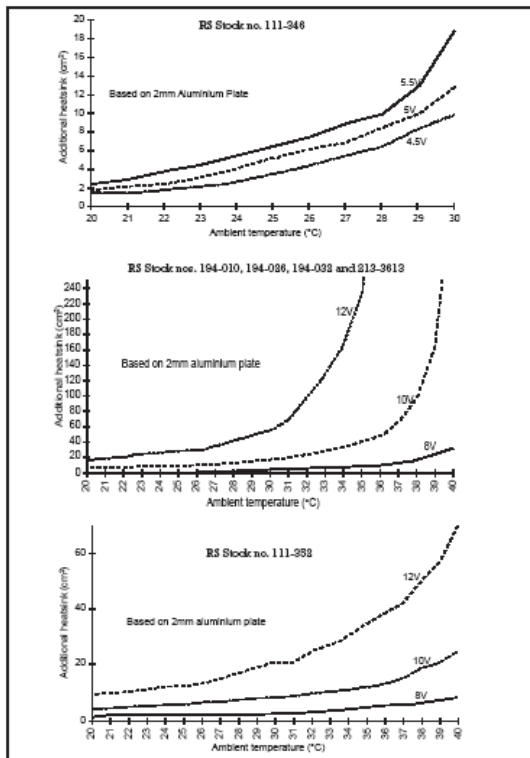
An input of between +4 and +7V applied to the TTL disable input will turn the laser 'off' and an input of 0V will turn it 'on'. If it is not in use it may be left floating. The laser may be pulsed 'on' and 'off' using this input to a frequency of at least 10Hz.

Heat sink requirements

When operating above their minimum supply voltage and/or at elevated temperatures above 30°C ambient, an additional heat sink must be used. If the case temperature of the embedded laser diode should exceed its maximum specification, premature or even catastrophic failure may occur.

To help dissipate heat from the laser modules the following graphs have been provided which show the additional surface area of 2mm thick aluminium plate required by each model when operated from different supply voltages and in different ambient temperatures. It has been assumed that good contact exists between the module and the additional heat sink to ensure low thermal resistance.

For maximum effect position, the heat sink so that it contacts the module just to the rear of the fluted front section (this may require peeling back the label) and use thermally conductive cream between surfaces.



When using a proprietary heat sink, the following equation may be used:

$$\varnothing_h \sim \frac{T_c - T_a}{I_{op} \times V_{op}} (\varnothing_m + \varnothing_c)$$

Where:

- \varnothing_h = Thermal resistance of additional heat sink (°C/W)
- \varnothing_m = Thermal resistance of laser module (°C/W)
- \varnothing_c = Thermal resistance of contact, module to heat sink (°C/W)
- T_c = Maximum operating case temperature for laser diode (°C)
- T_a = Maximum expected ambient temperature (°C)
- V_{op} = Operating voltage of laser module (V)
- I_{op} = Operating current @ V_{op} (A)

$\varnothing_m + \varnothing_c$ for these laser modules is typically 10°C/W assuming a good thermal contact between module and heat sink.

T_c is specified for each module as follows:

RS stock no.	°C
111-352	60
111-346	40
194-026	50
194-010	50
194-032	50
213-3613	50

Example:

If:

$\varnothing_m + \varnothing_c = 10$, $T_c = 50^\circ\text{C}$, $T_a = 35^\circ\text{C}$, $V_{op} = 10\text{V}$, $I_{op} = 78\text{mA}$

Then:

$$\varnothing_h \sim \frac{50 - 35}{0.078 \times 10} - 10$$

$$\sim 9.2^\circ\text{C/W}$$

Expected life

The laser diode device contained within each module, while being a semiconductor, is a complex electro-optical material, the structure of which determines the wavelength of the light emitted. The mechanism which ultimately causes the laser diode to fail is the formation of dislocations or gaps in the material structure. Laser devices which operate in the visible region of the spectrum have a more brittle structure than those that operate in the infra-red and in consequence produce dislocations at a faster rate.

The rate at which dislocations form during normal use is related to the temperature at which the laser diode operates. Where possible every means should be used to minimise temperature, such as working at lower voltage levels, reducing operating ambients and providing adequate heat sinking, all of which will contribute to maximise the operating life. The figures quoted for 'mean time to failure' (MTTF) reflect the differences in device structure and operating power.

Lasiris™ MFL Micro-Focus Laser

FEATURES

- Two year warranty
- Extremely thin lines down to 5.0 μm at $1/e^2$
- Wide range of wavelengths
- Uniform intensity distribution with line generator
- Superior mechanical stability
- ESD, over-temperature, over-voltage, and reverse-polarity protection
- Rugged stainless-steel housing



StockerYale's Lasiris™ MFL Micro-Focus lasers produce lines as thin as 5.0 μm at a specified working distance and are designed for applications where utmost accuracy and precision are required.

Our OEM customer base is constantly creating new applications that benefit from this technology, including medical and semiconductor applications such as inspection of microelectronics, biometrics, optical fiber alignment and inspection, high resolution 3-D contour mapping, and other machine vision applications.

Lasiris™ MFL lasers use patented uniform line generator optics. Our wide range of standard and custom models have exceptional mechanical stability, ESD protection, and feature a fully protected integrated laser diode driver.

A dot generator projecting an elliptical spot at a 1:3 ratio is also available.



APPLICATIONS

The MFL series was designed for applications that require the utmost accuracy and precision. Specific examples include:

- Precision inspection of small parts such as chips, wafers, small pins, resistors, semiconductor components
- Optical fiber alignment and inspection
- High precision surface analysis
- Machine vision
- 3-D contour mapping
- Industrial inspection
- Biometrics

OPTIONS AND CUSTOM UNITS

The laser is available with options allowing you to strobe or control its output electronically (refer to the Pulsing and Power Adjustment section). Please contact our application engineers for specific requests, since custom units can be built for specialized applications.

AVAILABLE PATTERNS

Single Line Single Dot

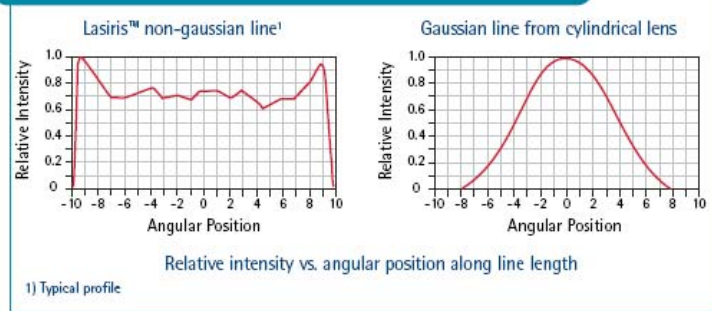


For multiple line or other patterns, please call us for details.

UNIFORM INTENSITY

Laser line patterns are often generated by cylindrical optics that produce a gaussian line profile with a bright center and fading ends. Lasiris™ patented optics spread the light into an evenly illuminated line. The result is crisp, uniform lines with sharp ends.

LINE INTENSITY PROFILE ALONG LINE LENGTH



LINE THICKNESS AND DEPTH-OF-FIELD

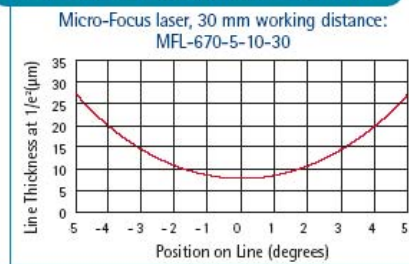
MFL lasers feature factory-set focusing for specific working distances. The table below shows the typical centerline thickness (at 1/e²) and depth-of-field performance of a 670 nm wavelength MFL. The depth-of-field is defined as twice the distance over which the thickness of the line has increased by a factor of √2.

NOMINAL WORKING DISTANCE	LINE THICKNESS** (± 1 MICRON)	DEPTH-OF-FIELD	MAXIMUM FAN ANGLE SUGGESTED*	LINE THICKNESS AT BOTH ENDS OF MAXIMUM FAN ANGLE
20 mm	5.0 μm	55 μm	5°	7 μm
30 mm	9 μm	140 μm	7.1°	12 μm
65 mm	13 μm	320 μm	7.1°	18 μm
90 mm	16 μm	510 μm	7.1°	22 μm
120 mm	19 μm	720 μm	7.1°	26 μm
185 mm	30 μm	1.7 mm	10°	42 μm

*If the requested fan angle is equal to the maximum fan angle suggested above, the thickness at both ends of the line will be a factor √2 thicker than at the center of the line. For example, a 13 μm line thickness at center will become: 13 μm x √2 = 18 μm at both ends of the 7.1° line.

**Line thickness is a function of angle divergence and wavelength. The larger the divergence and shorter the wavelength, the thinner the achievable line thickness. Please contact our sales engineers to receive a calculation for the laser and working distance of your choice.

THICKNESS VERSUS POSITION



LINE THICKNESS VERSUS POSITION ON LINE

The 'Thickness versus position' graph shows how the line thickness of the MFL laser increases farther away from the center of the line. Because of this unavoidable behavior we do not recommend the use of fan angles greater than those specified in the Line Thickness and Depth-of-Field section.

LASERS AND EYE SAFETY

Our lasers can comply with CDRH and IEC certification and fall in different safety classes depending on output power, wavelength and fan angle. According to CDRH 21CFR1040.10 regulations, they can be classified Class II, Class IIIa, or Class IIIb.

According to IEC 60825-1 regulations, they can be classified Class 1, 1M, 2, 2M, 3R, or 3B. For Class 1M and 2M lasers, viewing the laser output with certain optical instruments (magnifiers, binoculars, etc.) may pose an eye hazard.

Call us or visit our website for further details.



CAUTION: It is important to follow laser safety rules and wear appropriate protective eyewear when working around lasers. Use of controls, adjustments or performance of procedures other than those specified in the instruction manual may result in hazardous radiation exposure.

SPECIFICATIONS

MECHANICAL SPECIFICATIONS

Weight	175 g ±15 g
Dimensions	See dimensional diagrams
Housing material	Stainless steel

OPTICAL SPECIFICATIONS

Diode power	1 to 150 mW, varies with model
Wavelength	375 to 1550 nm, varies with model
Intensity distribution	Uniform (non-gaussian) for line, Gaussian for dot
Fan angles	1°, 5°, 7.1°, 10°, 15°, custom
Line thickness	Varies with model
Bore sighting	<3 mrad

ENVIRONMENTAL SPECIFICATIONS

Operating temperature	-10°C to +48°C
Wavelength drift	0.25 nm/°C typical
Thermal stability	Less than 5% change in focus over multiple temperature cycling from 10°C to 30°C
Over-temperature protection	Built-in: 48°C

ELECTRICAL SPECIFICATIONS: POWER SUPPLY

Input voltage	5 - 6 Vdc Optional 9,12,24 Vdc, 115/220 Vac
Connector type	Male phono-jack 3.5 mm Ø, or custom
Slow start time delay	10 µsec
Reverse-polarity protection, Over-voltage protection	

OPTIONS

POWER OPTIONS

Power Adjustment Potentiometer
The laser power can be easily changed by adjusting an optional built-in potentiometer with a small screwdriver. Indicate Code "P".

Pulsing Et Power Adjustment

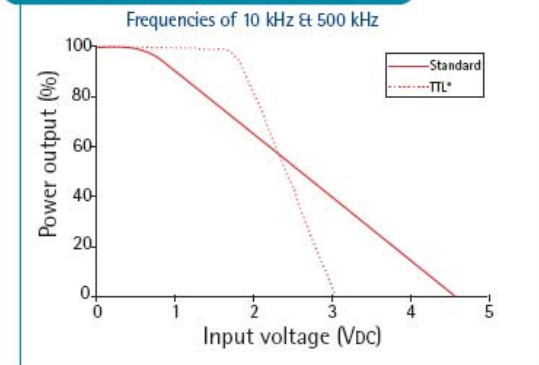
The power can be modulated or pulsed using an external signal. Input voltage of 0 Vdc: "on", 5 Vdc: "off" (or can be reversed). See figure below.

Coding:

- Standard S: 10 kHz FS*: 500 kHz
 - TTL T*: 10 kHz FT*: 500 kHz
- 2 MHz available.

Impedance	> 1 kΩ
Rise/Fall time	10 µsec for 10 kHz, 0.23 µsec for 500 kHz

POWER ADJUSTMENT CURVES



*Not available on all models.

The standard slope can be modified.

SEPARATE ELECTRONICS OPTION

The electronics of the laser can be separated. See diagram 'MFL laser with separate electronics option' on next page for details. Indicate Code "SD".

ORDERING INFORMATION

Micro-Focus lasers 635 to 1550 nm are covered under a 2-year warranty (parts & labor). To order, select from the specifications below. Code: MFL (or MFD for dot) - Wavelength & Power Option (if applicable) - Diode Power - Fan Angle (for line) - Working Distance - Separate Electronics option (if applicable; it is a standard for certain wavelength and diode power combinations). E.g., MFL-635S-35-1-20-SD, MFD-635-35-30, etc. Call us or visit our website for updates and other specifications.

STANDARD WAVELENGTHS AND DIODE POWERS

635 nm	1, 5, 10, 15, 35 mW
660 nm	1, 5, 10, 20, 35, 50, 80, 100 ^(a) mW
690 nm	20, 35 mW
785 nm	20, 35, 75 mW
830 nm	30, 100, 150 mW
Custom	

^(a) Please call us for details.

WORKING DISTANCE (660 NM)

20 mm ± 1 mm (5.0 μm focus)
30 mm ± 2 mm (9 μm focus)
65 mm ± 3 mm (13 μm focus)
90 mm ± 3 mm (16 μm focus)
120 mm ± 3 mm (19 μm focus)
185 mm ± 5 mm (30 μm focus)

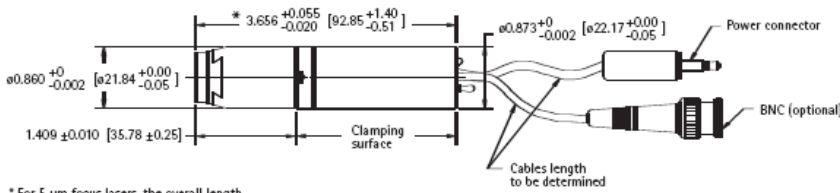
FAN ANGLE

1°
5°
7.1°
10°
15°
Custom

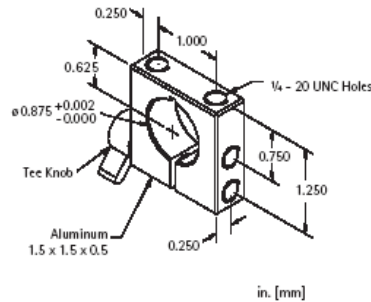
Please read section on line thickness and depth-of-field. For other wavelengths, the best focus is proportional to the wavelength.

Other wavelengths and diode powers are available. Please call us for more details.

DIMENSIONAL DIAGRAMS



M-875 MOUNTING BRACKET



Patents: US #4,826,299 / CAN #1,276,827 / Other patents pending

Information and specifications contained herein are deemed to be reliable and accurate. StockerYale reserves the right to change these specifications at any time without notice.



Vision Light Tech
 Protonenlaan 22
 NL-5405 NE ULDEN
 The Netherlands
 Telephones: +31 (0)413 260067
 Fax: +31 (0)413 260938
 Email: info@vlt.nl





LightWise Camera Series

**High Performance
Line Scan Module
FireWire™ / 1394a
Smart Digital Imaging Module
Featuring High Quality Linear 1K Sensor
and On-Camera Image Buffer**

LW-ELIS-1024A-1394

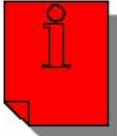


User's Guide

Version 2.2

*Copyright, 2003, Imaging Solutions Group of NY, Inc., All Rights Reserved
Version 2.2 Subject to change without notice.*

1 of 1



Important Note Regarding Grounding and ESD Protection:

We have observed some inconsistencies in 3rd party 1394 interface cards grounding strategy. Some 1394 cards do not ground the 1394 shield to chassis ground on the host computer, and some cards exhibit a “partial” ground. Some professional vision cards assume that the camera ground will be provided by the vision system or apparatus the camera is mounted to.

The ISG 1394 cameras require proper grounding and assume the 1394 cable shield provides a path to ground for the camera chassis. If this connection is faulty, the camera may exhibit an increased susceptibility to electro-static discharge. Please insure that the card you are using provides a ground path via the 1394 cable shield, or add a ground wire or other means to properly ground the camera.



Table of Contents:

- 1 LW-ELIS-1024 Introduction and Specification Overview**
 - 1.1 Product Description**
 - 1.2 Key Specifications**
 - 1.3 Panavision SVI ELIS Series Image Sensor**
 - 1.4 Programming and User Configuration Options**
 - 1.5 Automatic Gain and Offset Correction**
 - 1.6 Modes of Operation**
 - 1.7 Simplified Block Diagram**

- 2 External Signals and Connectors**
 - 2.1 External Connectors**
 - 2.2 Internal Connectors**
 - 2.3 Connector Pin Assignments**

- 3 Programming Guide**
 - 3.1 Interface**
 - 3.2 Memory Map and Register Definitions**

- 4 Mechanical Information**
 - 4.1 Lens Mount**
 - 4.2 Tripod Connection**
 - 4.3 Imager Module Dimensions**
 - 4.4 Evaluation Platform Dimensions**
 - 4.5 Module Components**

- 5 ISG Firmware + FPGA Upgrade Process**

*Copyright, 2003, Imaging Solutions Group of NY, Inc., All Rights Reserved
Version 2.2 Subject to change without notice.*

3 of 3



Section 1: LW-ELIS-1024 Introduction and Specification Overview

1.1 Product Description

The ISG Line Scan Imager Module provides a High performance Line Imager with high quality high-speed video with excellent response characteristics. The low cost and ease of integration into existing systems make it an excellent solution for a wide variety of applications. The interfaces to the Imager are industry standard to provide ease of integration into target systems. Applications include:

Automated Inspection Systems
 Bar Code Reading
 Machine Vision Systems
 Encoding and Positioning
 Parcel Scanning
 Programmable Smart Camera Applications

1.2 Key Specifications

- Linear Resolution: 1024 Pixels
- Data Rate: Up to 10 Mpixels / second
- Data Resolution: On-Board 14 bit A to D
- High Sensitivity and Wide Dynamic Range
- On-Board FPN Correction
- Standard FireWire™ (1394a) Interface (see TM note, page 23)
 Fully compliant to IEEE-1394a IIDC DCAM Specification Version 1.3
- Single 12V Supply
- Compact Form Factor
- User Programmable: *Integration Time, Multiple Gain Adjustments, Offset, Bit Depth, and Data Rate*
- Built-In Test Pattern
- External Trigger Option
- On-Board Image Buffer (16MB)
- On-Board FPGA for User-Configurability

*Copyright, 2003, Imaging Solutions Group of NY, Inc., All Rights Reserved
 Version 2.2 Subject to change without notice.*

4 of 4



1.3 Panavision SVI ELIS Series CMOS Image Sensor

The module utilizes the ELIS family of image sensors (see ELIS data sheets for detailed sensor information), which consists of an array of high performance, low dark current photo-diode pixels. The sensor features sample and hold capability, selectable resolution and advanced power management. Internal logic automatically reduces power consumption when lower resolution settings are selected. A low power standby mode is also available to reduce system power consumption when the imager is not in use.

1.4 Programming and User Configuration Options

The LW-ELIS-1024 offers several levels of programmability and user configurability. These include:

- Full Parameter Control, Set-Up and Operation Control via the **ISG Graphical User Interface Software**. This software is included with each unit.
- Parameter Control, Set-Up and Operation Control using software packages which support the **IIDC 1394-based Digital Camera Specification Version 1.30**. This includes vision packages by National Instruments, Matrox, Unibrain and many others.
- Full Parameter Control, Set-Up and Operation Control via **direct access of the module's register set**. Section 3 is the programmers' reference for this mode of operation.
- **Customization of on-board FPGA**. The on-board FPGA can be customized to include smart camera functionality, such as specialized image processing, data feature extraction, custom dynamic range mapping, etc. This method can also be used to configure the external I/O signals for custom functionality. Imaging Solutions Group is available for consulting with customers to enable custom configurations via the on-board FPGA. Contact sales@isgchips.com for information.

*Copyright, 2003, Imaging Solutions Group of NY, Inc., All Rights Reserved
Version 2.2 Subject to change without notice.*

5 of 5



1.5 Automatic Gain and Offset Correction

The LW-ELIS-1024 provides on-board FPN correction through gain and offset compensation. The FPGA algorithms in conjunction with an on-board dual 8-bit DAC perform automatic offset correction and semiautomatic gain corrections. These functions can be selected and activated by the provided ISG Graphical User Interface (GUI) software, or can be accessed directly via register programming.

1.6 On-Board Image Buffer

The camera provides on-board image buffering for up to three frames color or nine frames monochrome 16MB of image data. Combined with the module's flexible trigger modes, this image buffer enables capturing a sequence of frames at the maximum frame rate of the sensor, then transferring the frames at any available 1394 bandwidth.

1.7 Modes of Operation

The LW-ELIS-1024A can be programmed to run in two different modes depending on the application.

Standard Mode (Default Operation) - In this mode the sensor integration time is controlled by the amount of time the electronic shutter is active. The integration time is followed by readout, and then the process is repeated. This allows for very precise control of integration time, while trading off some sensitivity. A characteristic to note in this mode is that the dark current profile of each pixel will be different because the pixels near the end of the array will be read out later in time relative to when the pixel integration ended. Most applications will not be sensitive to this effect.

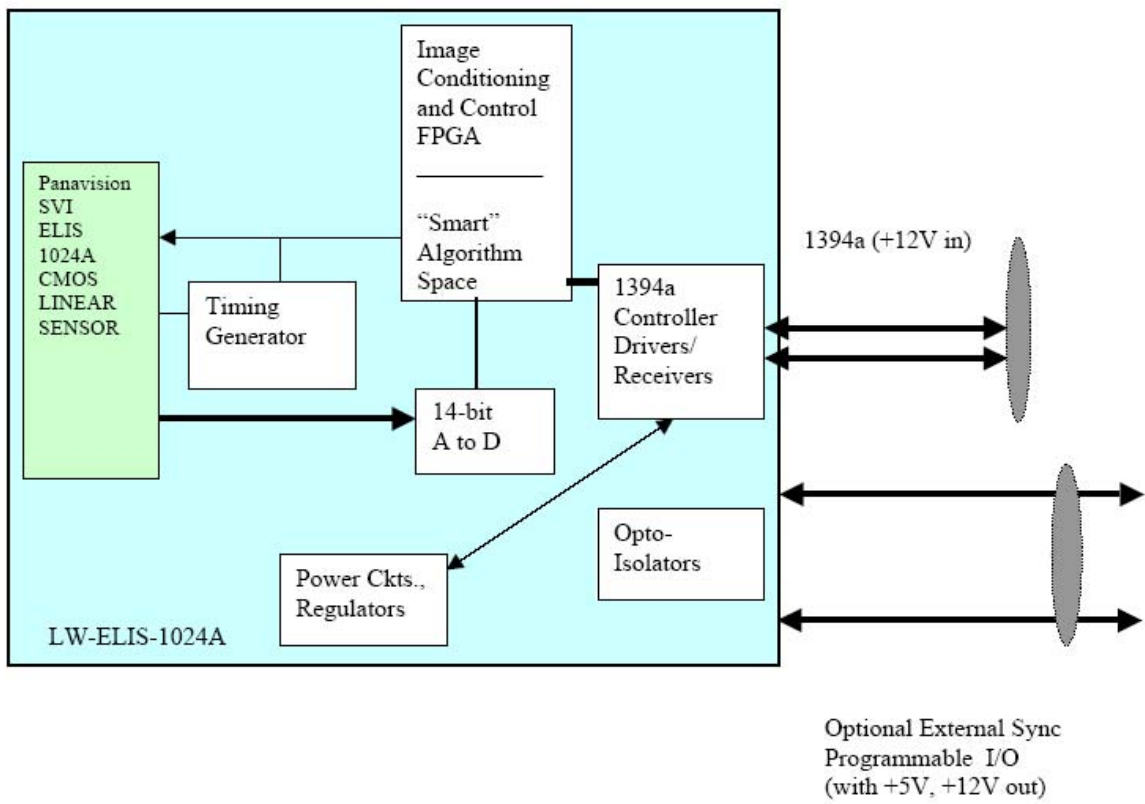
Dynamic Pixel Reset (DPR Mode) – In this mode each pixel is reset after read out and starts integrating immediately. An advantage to this mode is that every pixel is integrating for the entire line time (minus the one clock cycle for reset). A disadvantage is that the minimum integration time is driven by the readout time of the sensor (no electronic shutter). The integration time can be extended by adding a delay between line readouts (DPR Delay Register). DPR mode is available by setting ISG-defined registers via the 1394 interface. See table in Section 3.1.2.

*Copyright, 2003, Imaging Solutions Group of NY, Inc., All Rights Reserved
Version 2.2 Subject to change without notice.*

6 of 6



1.8 Simplified Block Diagram



Copyright, 2003, Imaging Solutions Group of NY, Inc., All Rights Reserved
 Version 2.2 Subject to change without notice.
 7 of 7



Section 2: Connectors and Trigger Modes

The ISG linear cameras can be triggered in frame or line rate modes or a combination of the two. The frame rate trigger (described in section 2.1) controls when the lines that make up a frame begin to be acquired. The line rate trigger (described in section 2.2) controls the interval between each line read out of the imager. It is possible to use both types of triggers simultaneously as long as the opto-isolate trigger input is used for the frame trigger and the differential trigger input is used for the line rate trigger. When not using line rate triggering either the differential or opto-isolated input can be used for frame triggering.

Section 2.1: Frame Trigger Description

Register Description:

Trigger Delay – A 16 bit value used to delay the start of image acquisition from the active edge of the input trigger. This value can be programmed in steps of 20.83 μ s to a maximum value of 1.37s.

Strobe Advance – This 8 bit register is used to apply the strobe signal a programmed amount of time before the start of image acquisition to allow for illumination turn on time. This value can be programmed in steps of 5.21 μ s to a maximum value of 1.33ms. Note: The trigger delay must be greater than the strobe advance.

Strobe Delay – This 18 bit register is used to delay the strobe signal a programmed amount of time after the start of image acquisition. This delay is intended for use with flash illumination devices. This value can be programmed in steps of .65 μ s to a maximum value of 170 ms. Note: The strobe delay must not exceed the image acquisition time. If a value is programmed for Strobe Advance the Strobe Delay value will be ignored.

Retrigger Delay – The 16 bit value in this register is used to program the time between image acquisition intervals when in Retrigger Mode. This value can be programmed in steps of 5.2 μ s to a maximum value of 341ms.

Strobe Duration - This register is used to program the duration of the strobe pulse when strobe duration mode is enabled. This value can be programmed in steps of 5.2 μ s to a maximum value of 341ms. Note: The strobe output will go inactive at the end of image acquisition no matter what the strobe duration is set to.

Trigger and Strobe Description:

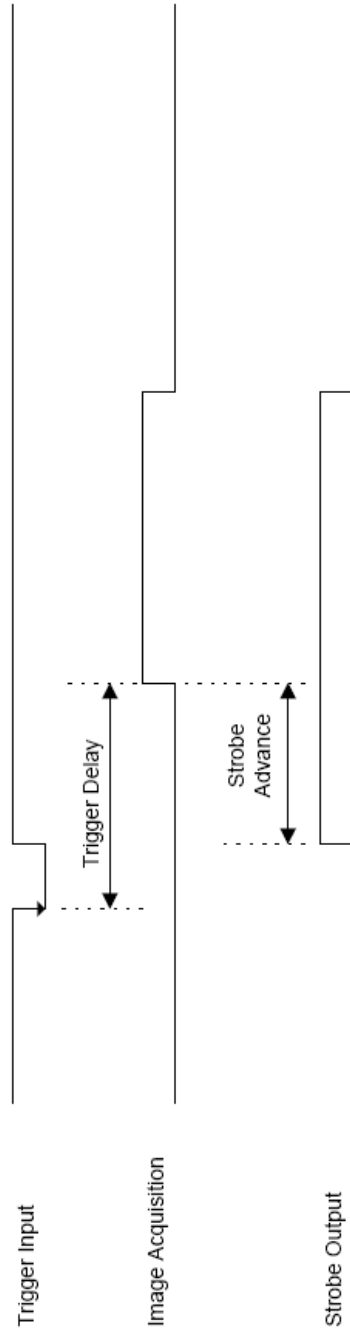
The input trigger sense can be active low or high. A software trigger is also available to the programming interface (Host Mode) as well as a trigger status bit. The strobe output is intended to control an illumination system and can be selected to be active low or high as well as always high or always low. The diagrams on the following pages show the trigger as active low and the strobe as active high.

*Copyright, 2003, Imaging Solutions Group of NY, Inc., All Rights Reserved
Version 2.2 Subject to change without notice.*

8 of 8



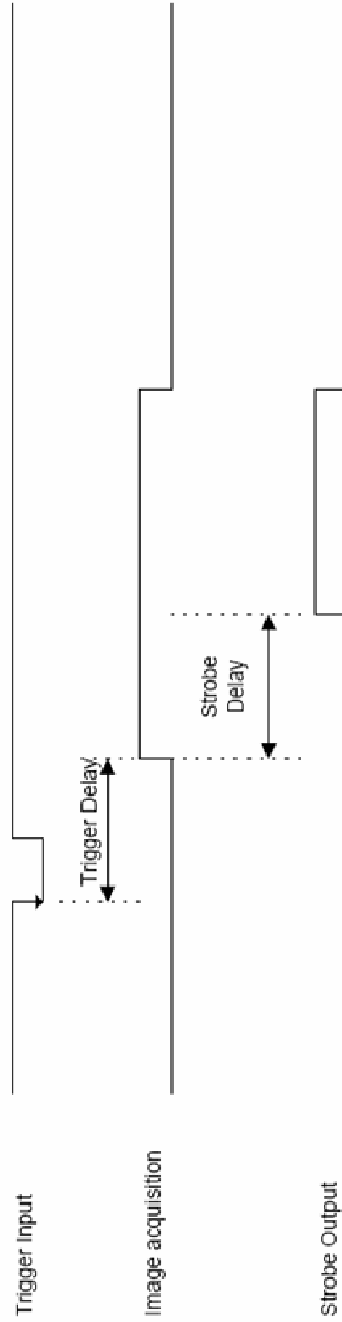
Trigger Mode A = IIDC Trigger Mode 0
Strobe Advance Shown



Copyright, 2003, Imaging Solutions Group of NY, Inc., All Rights Reserved
Version 2.2 Subject to change without notice.

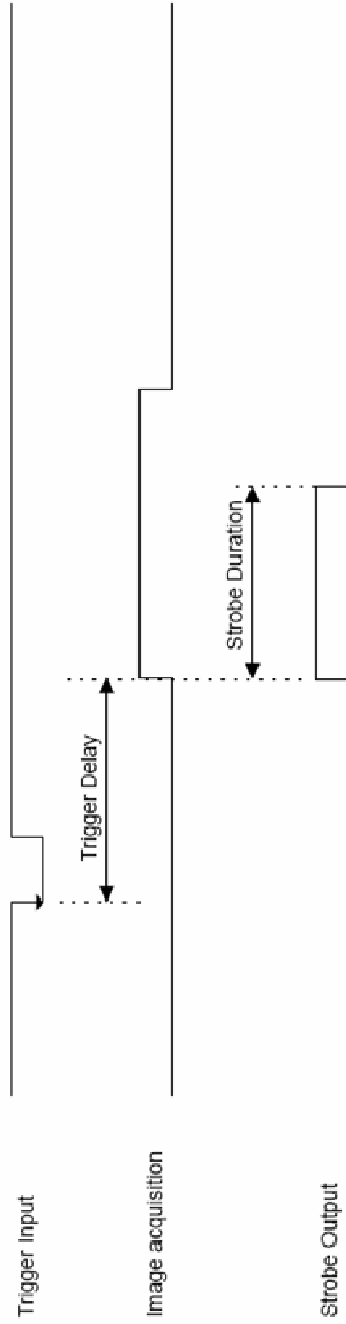


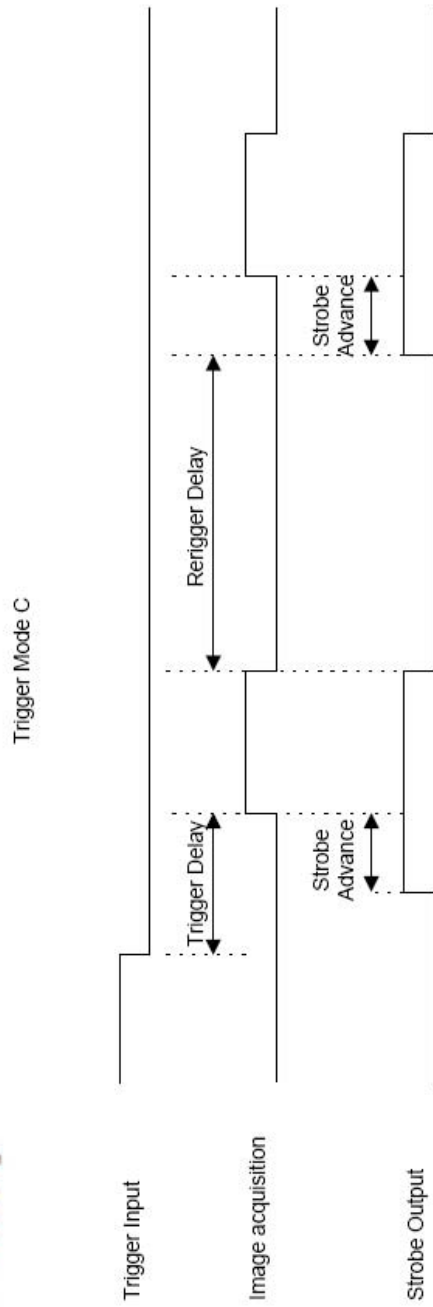
Trigger Mode A = IIDC Trigger Mode 0
Strobe Delay Shown





Trigger Mode A = IIDC Trigger Mode 0
Strobe Duration Shown





Copyright, 2003, Imaging Solutions Group of NY, Inc., All Rights Reserved
 Version 2.2 Subject to change without notice.
 12 of 12



Section 2.2: Line Rate Trigger Description

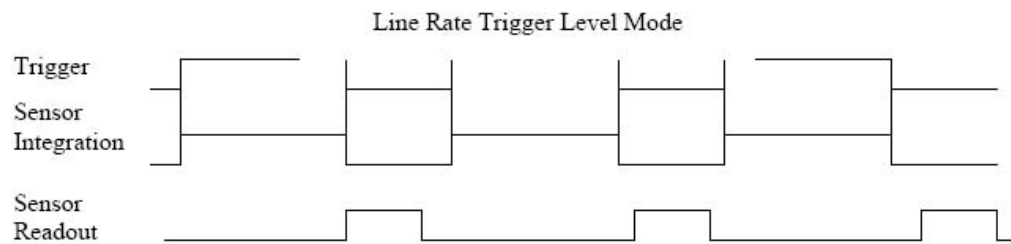
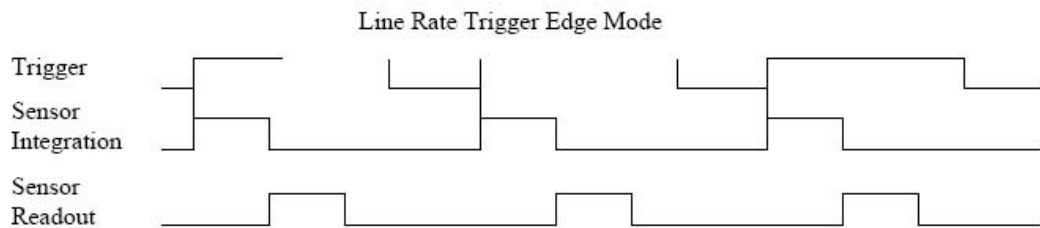
The line rate trigger is offered for applications such as web inspection where synchronization between the imaged target and the sensor line rate are required to maintain proper image aspect ratio. This is accomplished by feeding a differential signal from the tach to the differential trigger input. Two line scan modes are provided and can be enabled with bits 11 and 10 of the LISCR (0x424).

LISCR[11:10] 00 = Line rate trigger disabled.

LISCR[11:10] 01 = Line rate trigger enabled in edge mode.

LISCR[11:10] 10 = Line rate trigger enabled in level mode.

When using edge mode, the integration time is controlled with the shutter register as it is when not using line rate triggering. When using level mode, the line integration is controlled by the trigger active time. In other words the pulse width of the trigger input will control sensor integration time. Both modes are illustrated below.



*Copyright, 2003, Imaging Solutions Group of NY, Inc., All Rights Reserved
Version 2.2 Subject to change without notice.*

13 of 13



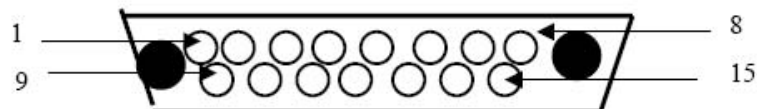
2.2 External Connectors

2.2.1 Firewire™ Connector: This interface is based on the industry standard 1394a specification. Two connectors are provided to allow camera daisy chaining.

2.2.2 15-position D-SUB I/O Connector:

- Connector part number: Molex part number 83612-9020
- Thumb Screw part number: Molex MDSM – 9PE-Z10-VR25
- Recommended Cable: Molex CA 83422-9014

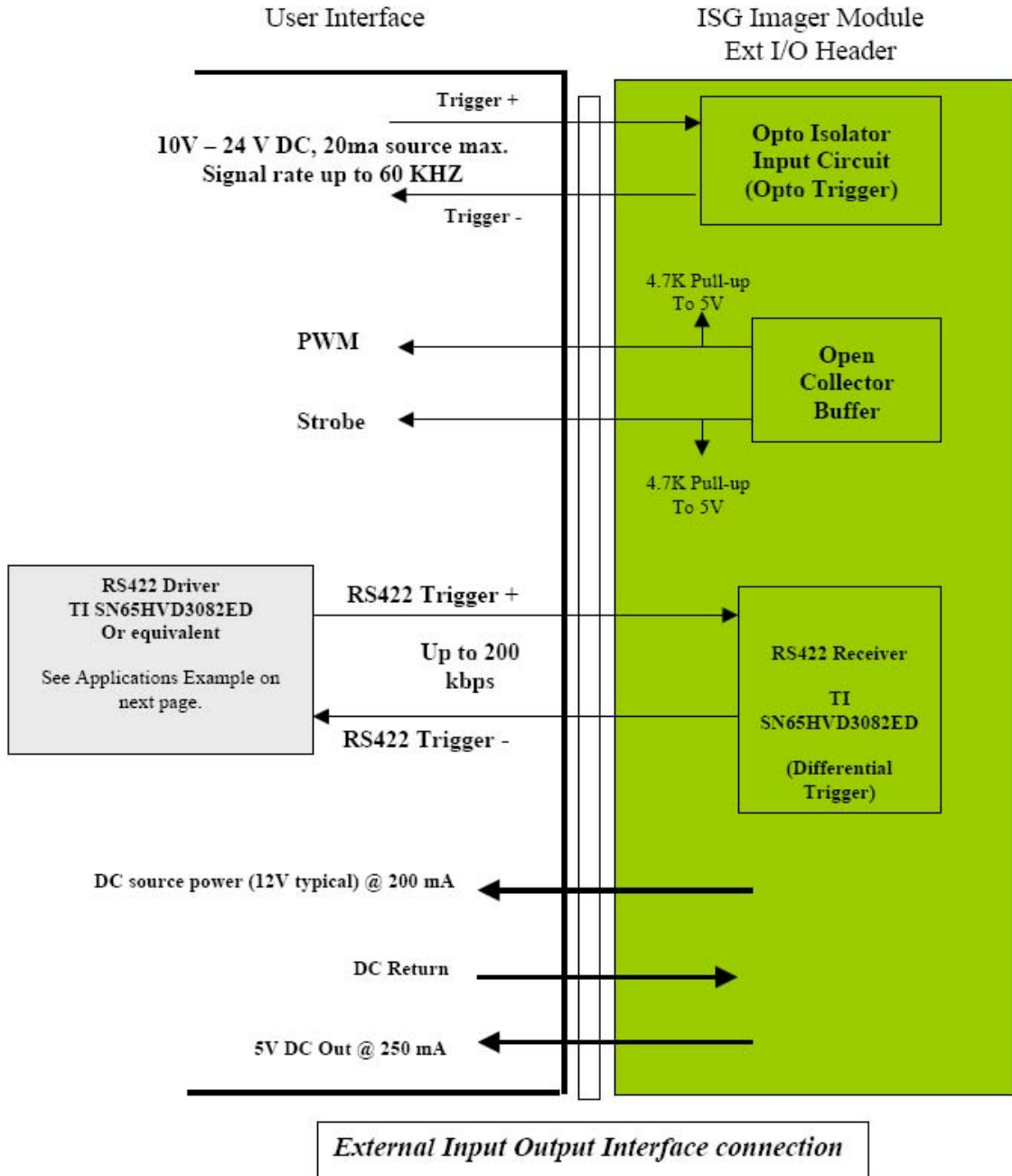
Pin	Function	Input/Output Type
1	Trigger +	Optoisolated Input
2	Trigger -	Optoisolated Input
3	GND	
4	DC Input (Optional)	Power Input
5	Strobe	Open Collector Output
6	Programmable PWM	Open Collector Output
7	GND	
8	DC Input (Optional)	Power Input
9	RS422 Trigger +	Diff. TTL Input
10	RS422 Trigger -	Diff. TTL Input
11	DC +5V Output	Power Output
12	Programmable Output +	Optoisolated Output
13	Programmable Output -	Optoisolated Output
14	Reserved	
15	GND	



15-pin Micro-D EXT IO Connector, Front View

Copyright, 2003, Imaging Solutions Group of NY, Inc., All Rights Reserved
Version 2.2 Subject to change without notice.

14 of 14



Copyright, 2003, Imaging Solutions Group of NY, Inc., All Rights Reserved
Version 2.2 Subject to change without notice.



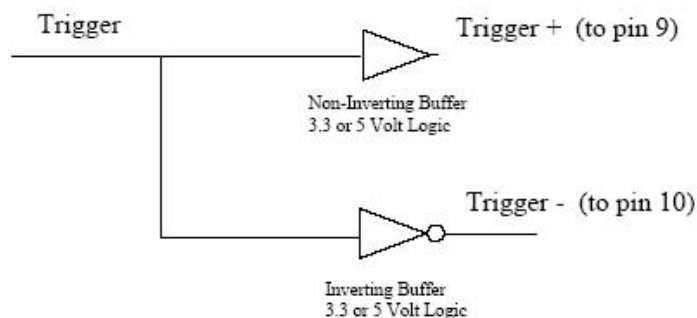
Applications Example: Using The RS422 Trigger Input

1) Preferred Method – RS422 Driver

The optimal way to utilize this input to trigger the camera is to drive the RS422 Receiver in the camera with the corresponding driver device. The recommended driver is TI part number SN65HVD3082ED. This method provides a balanced, robust differential input.

2) Alternate Method - Driving the RS422 Trigger Input with Standard 3.3 or 5 Volt CMOS/TTL Logic

Standard digital logic can be used to simulate a differential signal and trigger the camera using the RS422 input. This can be accomplished by generating a 3.3 or 5 Volt logic signal for RS422 Trigger +, and providing a logically inverted output of this signal for RS422 Trigger -. The following diagram illustrates this approach:



*Copyright, 2003, Imaging Solutions Group of NY, Inc., All Rights Reserved
Version 2.2 Subject to change without notice.*

16 of 16



Section 3: Programming Guide

3.1 Top Level Memory Map: All addresses are offset from address 0x7000

Sensor Map 0x000 - 0x3ff B12

Sensor Interface

SICR	0x400	B15	Sensor Interface Control (Control Register1)
SISTAT	0x404		Sensor Interface Status
TRGDLY	0x408	U16	Trigger Delay
STRBDLY	0x40C	U16	Strobe Delay
RTGDLY	0x410	U16	Retrigger Delay
PWM	0x414	U8	PWM Duty Cycle
STRADV	0x418	U8	Strobe Advance
STRDUR	0x41C	U16	Strobe Duration
ILISCR	0x424	B10	Linear Control Register (Control Register2)
SHUTTER	0x428	U16	Shutter Value (LGINT on SLIS)
NUM_ROWS	0x42C	U16	Number of rows in a frame
VV_STRT	0x430	U12	Start of line ROI
VV_END	0x434	U12	End of line ROI
INT_COUNT_VAL	0x43C	U11	Short Integration for SLIS
NDRO_COUNT	0x440	U8	NDRO Line count (ELIS Only)
DPR_DLY	0x444	U16	DPR delay (ELIS Only)
CLKCR	0x448	U5	Clock Divider/Control
PWM_SF	0x44C	U8	PWM Scale Factor
LRT_MULT	0x450	U9	Line Rate Multiplier

Image Path Control

IPCR	0x800	B14	Image Path Control
IPSTAT	0x804	B2	Image Path Status
HISTCOLSTRT	0x808	U12	Histogram Window Column Start
HISTCOLWIDTH	0x80C	U12	Histogram Window Column Width
HISTROWSTRT	0x810	U11	Histogram Window Row Start
HISTROWDEPTH	0x814	U11	Histogram Window Row Depth
HISTCR	0x818	B4	Histogram Control
HISTADDR	0x81C	U5	Histogram Address
HISTDATA	0x820	U26	Histogram Data
DGAIN	0x824	U4.4	Digital Gain
LUTADDR	0x8B4	U10	Look Up Table Address
LUTDATA	0x8B8	U10	Look Up Table Data
DOFF	0x918	U14	Digital Offset

*Copyright, 2003, Imaging Solutions Group of NY, Inc., All Rights Reserved
Version 2.2 Subject to change without notice.*

17 of 17



3.2 Register Detail

Please contact ISG for register programming details.

Section 4: Mechanical Information

4.1 Lens Mount

A Case-Mount CS type (1.0" diameters with 12.5 mm spacing between the surface of the sensor and top of the lens-mount) lens mount is provided for both system configurations.

C-Type Lenses: A five mm extender will change the CS to C-Type lens mount with 17.5 mm Back Focal Length.

F-Type Lenses: Using the Cannon 50mm F-type FD series + the Cannon "C-type to F-type" adapter will convert the camera to F-type with 39.9 mm Back Focal Length.

4.2 Tripod Connection

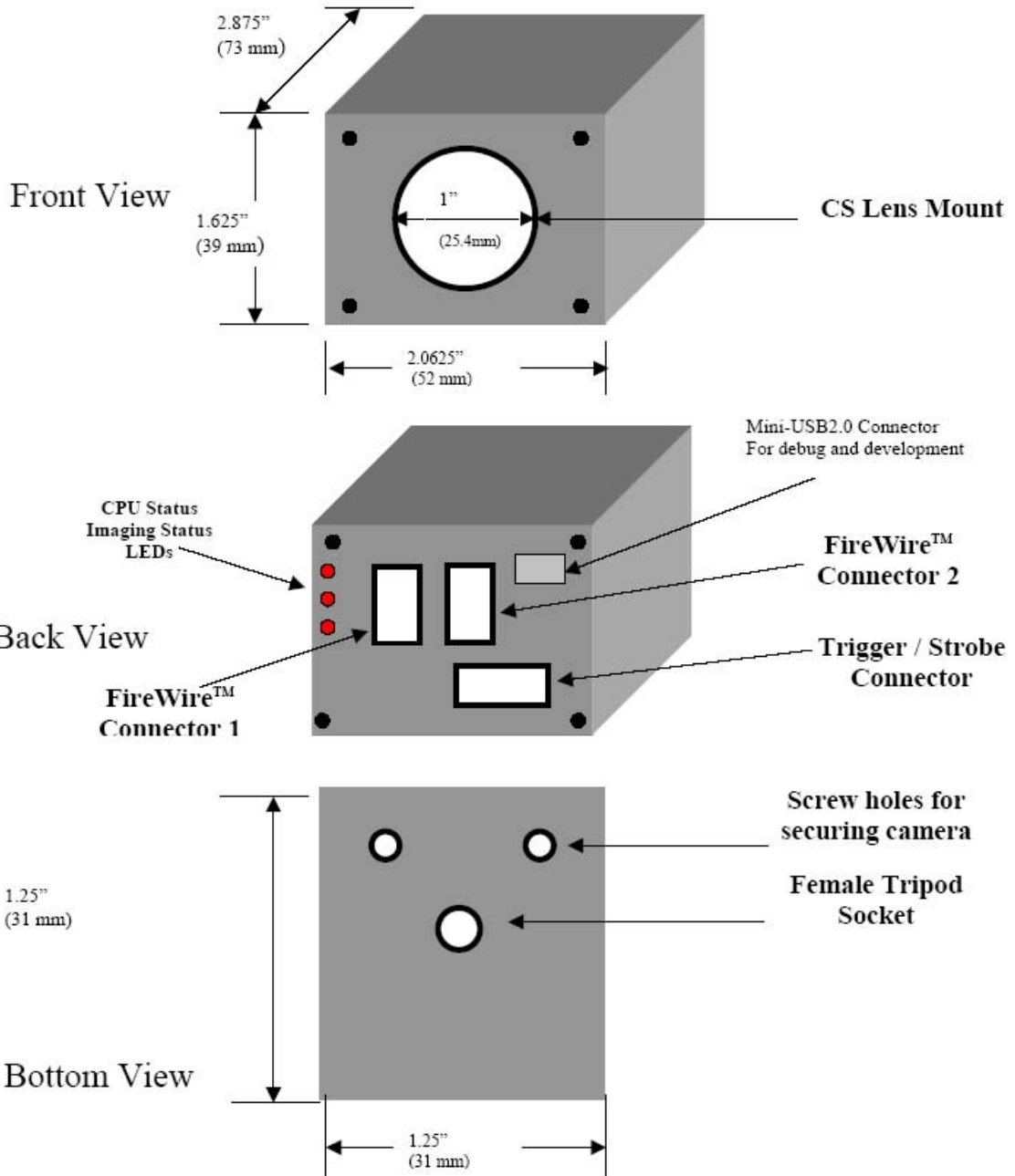
A standard female tripod connection is provided at the bottom of the Imager module and the Evaluation platform

*Copyright, 2003, Imaging Solutions Group of NY, Inc., All Rights Reserved
Version 2.2 Subject to change without notice.*

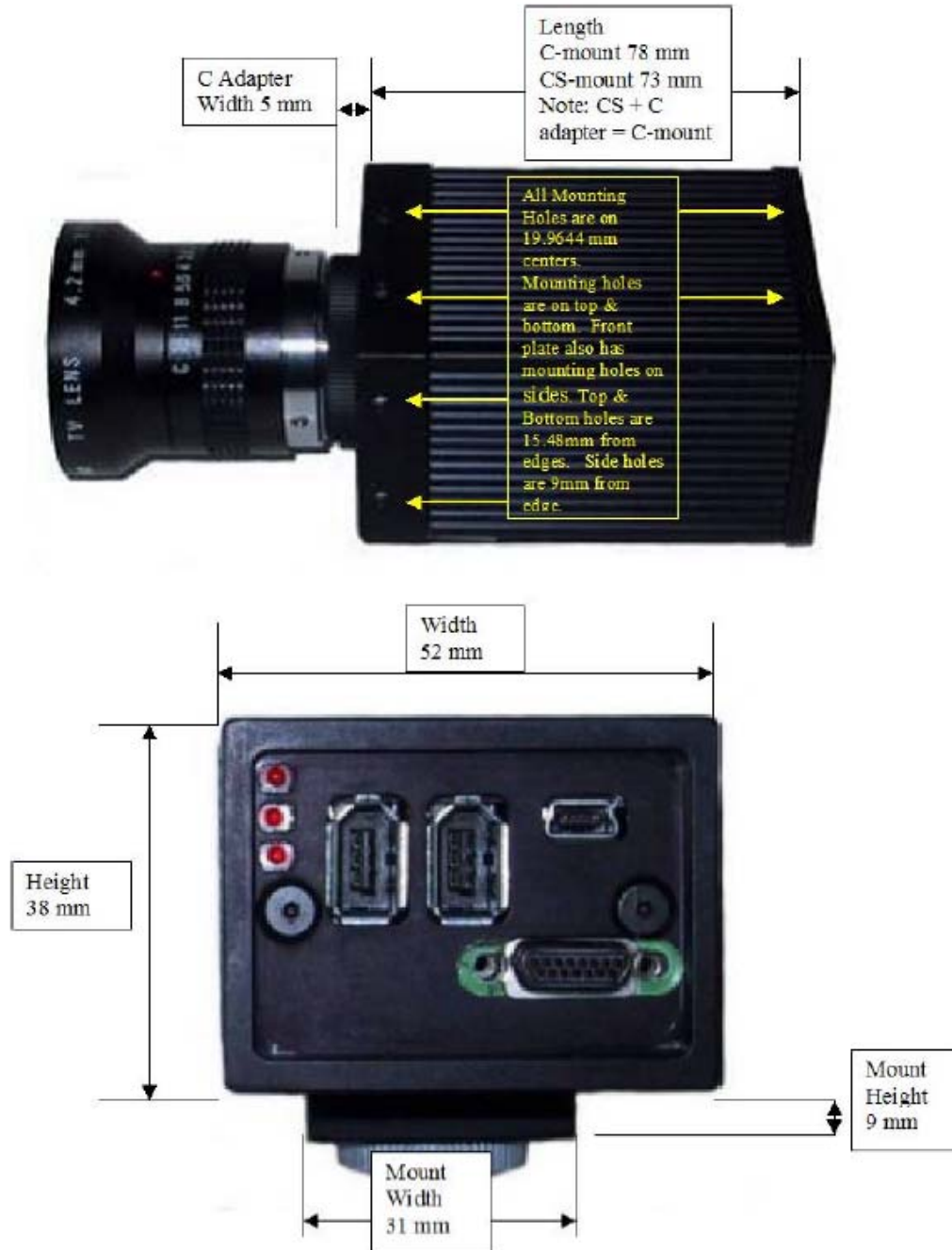
18 of 18



4.3 LW-ELIS-1024A-1394 Line Scan Module Dimensions



Copyright, 2003 Imaging Solutions Group of NY, Inc., All Rights Reserved
 Revision 1.0 Subject to change without notice.
 19 of 19



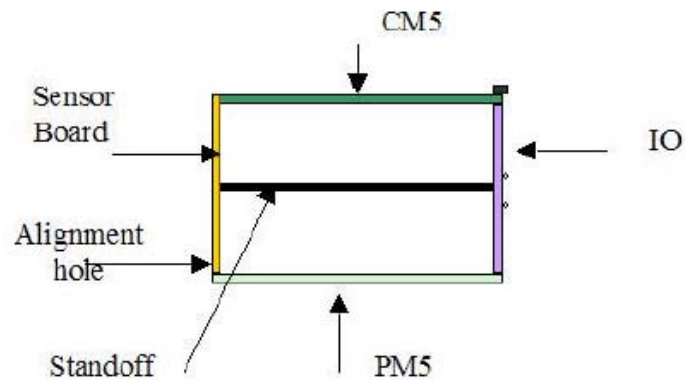
Copyright, 2003 Imaging Solutions Group of NY, Inc., All Rights Reserved
 Revision 1.0 Subject to change without notice.
 20 of 20



4.4 Module Components:

The ISG LW-ELIS-1024A-1394 Line Scan Module hardware design is partitioned into four separate boards: 1) Sensor, 2) Controller 3) I/O board and 4) Power Management boards. These boards are SMT type 2 (double sides) and are connected to each others as shown below:

The module electronics consists of 4 boards: Sensor, Controller (CM5), Power Management Board (PM5) and the IO board.



*Copyright, 2003 Imaging Solutions Group of NY, Inc., All Rights Reserved
Revision 1.0 Subject to change without notice.*

21 of 21



4.5 Operating Conditions

Measured Average Power Consumption via 1394 cable:
12V, 250 ma rms / 3.0W

Ambient Operating Temperature Range:
-10 to 45 C

FCC and CE Qualification: In progress.
Test results available upon request.

Vibration and Shock Testing: In progress.
Target specification: 7G rms (10Hz to 2000Hz) Random, Shock
70G. Test results available upon request.

5.0 ISG Firmware + FPGA Upgrade Process

This process will use the ISG Camera Control GUI application software on the host PC, to update firmware and/or FPGA code on the ISG 1394 camera. The camera's firmware/FPGA code is loaded through the 1394 interface using the ISG GUI.

A customer wishing to do a firmware or FPGA upgrade should perform the following steps:

1) Extract, and copy the firmware/FPGA binary data files to a directory on your host PC. The files are named isgcpu_ccxx_xxxx.bin for updating the camera firmware, and isgfpga_ccxx_xxxx.bin for updating the camera hardware (i.e. FPGA device code). The ccxx field represents the camera type, and the xxxx field will hold the version number.

*Copyright,2003 Imaging Solutions Group of NY, Inc., All Rights Reserved
Revision 1.0 Subject to change without notice.*

22 of 22



- 2) To upgrade the firmware on the camera, start by running the ISG Lightwise GUI. Note that the ISG supplied driver for the camera must be installed in order to use the ISG GUI. It is recommended that the camera viewer window be closed before continuing.
- 3) Click on the "Camera Control Dialog" button on the ISG GUI.
- 4) Select the "Camera Setup" tab from the Camera Control Dialog page. The Camera Setup page can be used to update either the firmware or the FPGA code of the camera, or both.
- 5) Use the browse button (labeled "...") to search for and select either the isgcpu or isgfpga binary file defined in step 1 above, depending on which part of the camera you are updating.
- 6) To begin the actual download procedure, click on the "Download to CPU" or "Download to HW" button as appropriate. A popup box will ask if you are sure that you want to continue the process.
- 7) Confirm that you are sure you want to proceed with the upgrade by answering, "yes" within the confirmation popup dialog. Once confirmed, insure that this process is not interrupted (i.e. maintain 1394 cable connection). The progress bar will show the status of the update. Note that an FPGA update will take a few minutes to complete. The process is completed once the dialog states "Done" on the download button. At this point, the camera is upgraded with new firmware/FPGA code.
- 8) Exit the GUI. Power cycle the camera by disconnecting and reconnecting the 1394 cable to allow the new code to be executed.
- 9). After the camera is connected, you can right click in the top toolbar of the GUI and select "about isg camera system" to read the new version numbers.

Trade Mark Note:

FireWire™ is a registered trademark of Apple Inc

*Copyright,2003 Imaging Solutions Group of NY, Inc., All Rights Reserved
Revision 1.0 Subject to change without notice.*

23 of 23

Line Scan Camera	Specifications
	LW-ELIS-1024a-1394
Imaging Device:	Linear CMOS
Sensing Area:	8.0 mm x 125 microns
Pixel Size:	7.8 micron x 125 micron Rectangular
Pixels (H x V):	1024 x 1
Pixel Depth:	14-bit
On-Board Image Buffer	16 Megabytes
Camera Control:	Via Software
Line Scan Rate:	10K lines per second
Pixel clock:	10 MHz
Synchronization:	External or via software
S/N Ratio:	> 80 db
Video Output:	FireWire™ IEEE-1394
Lens Mount:	C or CS-Mount
Mounting:	Via ¼-20 mounting adapter
Power Requirement:	Via FireWire™ 1394 Cable
Vibration (10-2K Hz):	7G
Shock:	70G
Dimensions (HxWxL):	38mm x 51mm x 72mm
Weight:	176g
Operating Temp.:	-10° C to 45° C
Pricing:	Call ISG or Edmund Optics

FOR MORE INFORMATION CONTACT:

Keystone Automation Inc., 5649 Memorial Avenue North, Stillwater, MN 55082
TEL: 651-439-4268 FAX: 651-439-4279 www.keystoneautomation.com

AVIIVA M2 IMAGING

AVIIVA™ M2 LINESCAN CAMERA

AVIIVA™
easy,
VERSATILE
and accurate



Key Features

- Sensor range : 512 to 4096 pixels
10 or 14 μm
- Interface : Camera Link or LVDS
- Mechanics : Compact, versatile
and accurate design
- Excellent Signal/Noise Ratio
- Data rate : up to 80MHz (scalable)
- Dynamic range : up to 12 bits (scalable)
- Other programmable settings :
 - * synchronisation mode
 - * clock selection

Typical applications

- Web inspection (printing, textile, paper...)
- Parts inspection or sorting
(food, pharma, container...)
- Surface inspection
(semiconductor, PCB, CD...)
- OCR and bar codes reading
(document scanning, postal sorting...)
- 3D metrology



AVIIVA M2 LINESCAN CAMERA

Corporate Headquarters

2325 Orchard Parkway
San Jose, CA 95131
USA
Tel: 1(408) 441-0311
Fax: 1(408) 487-2600

Europe

Atmel Sarl
Route des Arsenaux 41
Case Postale 80
CH-1705 Fribourg
Switzerland
Tel: (41) 26-426-5555
Fax: (41) 26-426-5500

Asia

Room 1219
Chinachem Golden Plaza
77 Mody Road Tsimshatsui
East Kowloon
Hong Kong
Tel: (852) 2721-8778
Fax: (852) 2722-1369

Japan

9F, Tonetsu Shinkawa Bldg.
1-24-8 Shinkawa
Chuo-ku, Tokyo 104-0033
Japan
Tel: (81) 3-3523-3551
Fax: (81) 3-3523-7581

**Biometrics/Imaging/Hi-Res MPU/
High Speed Converters/RF Datacom**

Avenue de Rochepleine
BP 123
38521 Saint-Egreve Cedex, France
Tel: (33) 4-76-58-30-00
Fax: (33) 4-76-58-34-80

E-mail

literature@atmel.com

Web Site

http://www.atmel.com



© Atmel Corporation 2002.
Atmel Corporation makes no warranty for the use of its products, other than those expressly contained in the Company's standard warranty which is detailed in Atmel's Terms and Conditions located on the Company's web site. The Company assumes no responsibility for any errors which may appear in this document, reserves the right to change devices or specifications detailed herein at any time without notice, and does not make any commitment to update the information contained herein. No licenses to patents or other intellectual property of Atmel are granted by the Company in connection with the sale of Atmel products, expressly or by implication. Atmel's products are not authorized for use as critical components in life support devices or systems.
Ref: 21683A/IMAGE-0802 5M



DETAILED SPECIFICATIONS

Sensor characteristics at maximum pixel rate					
Resolution	pixels	512	1024	2048	4096
Pixel size (square)	µm	14	14 or 10	14 or 10	10
Max Line rate	kHz	109	57	29	15
Anti blooming		x 150			

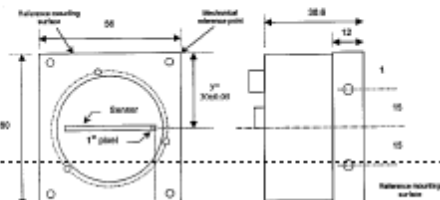
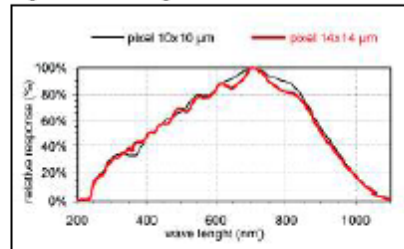


Radiometric performance at maximum pixel rate				
Dynamic range	bits	12 (also configurable in 8 or 10)		
Spectral range	nm	250 - 1100		
Non-linearity	%	< 1		
Gain range (step of 1.05 dB)	dB	Gain 0	Gain 16	Gain 20
Peak response pixel of 14µm	LRA/µm²	130	1040	4160
Peak response pixel of 10µm	LRA/µm²	50	499	1660
Output RMS noise (typical)	e-	67.4	46	37
SNR	dB	15.2	5.2	5.2
Input RMS Noise (typical) pixel of 14µm	µV/cm²	14		
Input RMS Noise (typical) pixel of 10µm	µV/cm²	37		

Mechanical & electrical interface	
Size (w x h x l)	mm 56 x 80 x 35
Lens mount	C (up to 1024 pixels); F; K
Sensor alignment	AXY=±50µm Z=±30µm XY=±20µm Z=±25µm
Outputs	3 x 12-bit digital outputs
Power supply	V single 1.2 to 2.4
Power dissipation	W < 9
Operating temperature	°C 0 to 55 (non condensing)
Storage temperature	°C 0 to 75 (non condensing)

Functionalities	
Dark level	automatic correction
Gain Offset	programmable
Integration time	by control interface
Clock selection	
External trigger / free run	
Line/field synchronization	
Regularity	CE and FCC compliant

Spectral Response



Connectors and data interface

Camera Link version	
Power connector	HR10 6-pin
Control connector	MDR 26 Camera Link
Data connector	shared with control
Programmable data rate	MHz 1@60, 1@40, 1@30, 1@20, 2@30, 2@20

LVDS version	
Power connector	HR10 6-pin
Control connector	RS 232 D-Sub 9-pin
Data connector 1	D-Sub HD 44-pin
Data connector 2(*)	D-Sub HD 26-pin
Programmable data rate	MHz 1@60, 1@40, 1@30, 1@20, 2@30, 2@20, 2@15, 2@10

(*) not used in 1@ mode and in 8 bits configuration



OVERVIEW OF ATMEL LINESCAN CAMERA OFFER

Commercial Name	M/C	Max Data Rate M Pixels/s	Interface	Resolution	Data Format
AVIIVA M2	Monochrome	60	CL/LVDS	512-1024-2048 4096	up to 12 bits
AVIIVA M4	Monochrome	160	CL	2048-6144-8192	up to 10 bits
AVIIVA C2	Color	60	CL/LVDS	4096	up to 12 bits
AKYLA MD20*	Color	3 x 20	CL/LVDS	1024-2048	up to 10 bits
AKYLA MD30*	Color	3 x 30	CL/LVDS	1024-2048	up to 10 bits

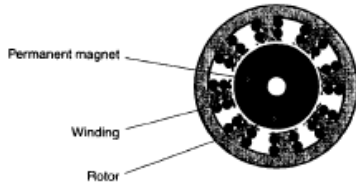
* with beam splitter

BRUSHLESS range from CROUZET

1 - Composition

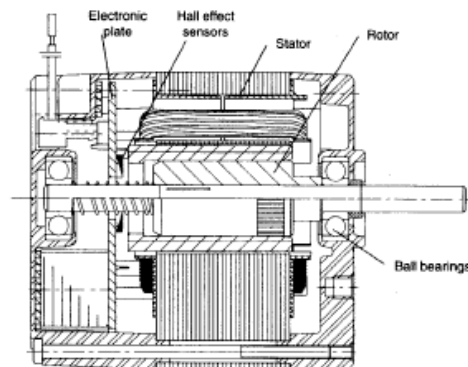
This new product range is based on the 3-phase motor with **internal rotor**. The high-energy plasto-ferrite magnet is completely integral with the motor shaft. The chosen structure gives high dynamic performance : made possible by the low inertia of the rotor (unlike motors with external rotors, which have high inertia) . The stator lamination stack acts as a heat dissipator for energy losses induced by the winding.

■ **Motor principle :**
With internal rotor,



Both zamac flanges mounted on the stator lamination stack are fitted with a ball bearing, ensuring the motor will have a long service life.

■ **Composition :**



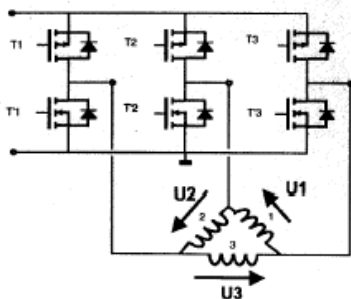
The electronics required for operation are completely integrated in the motor.

2 - Operating principle

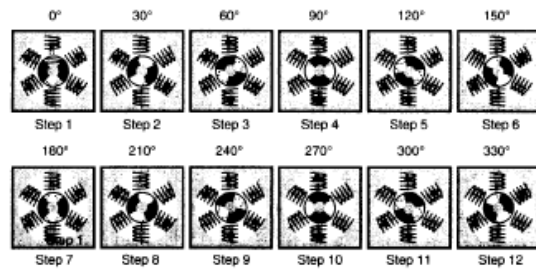
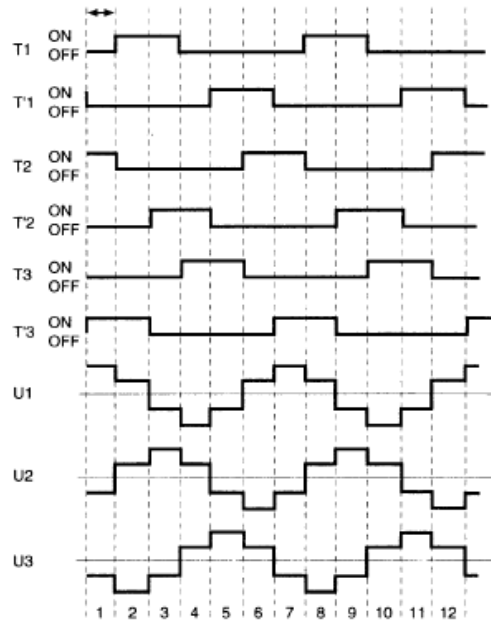
The chosen architecture is based on a "3-phase" motor, with a 4-pole rotor.

■ **Sequencing :** the "3-phase" motor is wired as "delta". Three hall effect sensors are used to locate the position of the rotor.

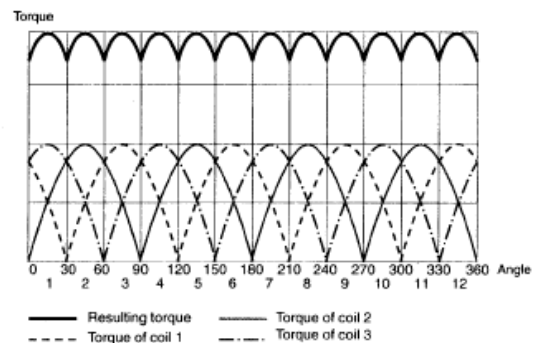
The transistors conduct up to 120°



Communication logic



Resulting torque form

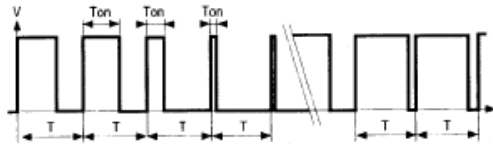


The "3-phase" motor provides the best possible compromise in terms of regularity of the resulting torque (low ripple percentage). As the electronics are completely integrated, all the sequencing is performed by the electronics inside the motor.



3 - Functions and inputs/outputs

The speed of the motors offered with integrated electronics can be controlled : by an analogue (0 - 10 volts), or digital (PWM : 15 kHz) speed signal.



■ Definition of PWM

T is constant, but Ton varies ; the Ton/T ratio is the cyclical ratio (as a %).

In this case, PWM is a control signal, converted by the electronics to set the speed.

- If the cyclical ratio is 0%, the speed is 0 rpm.
- If the cyclical ratio is 100%, the speed is N0 (no-load speed).
- If the cyclical ratio is 50%, the speed is N0/2 (half the no-load speed).

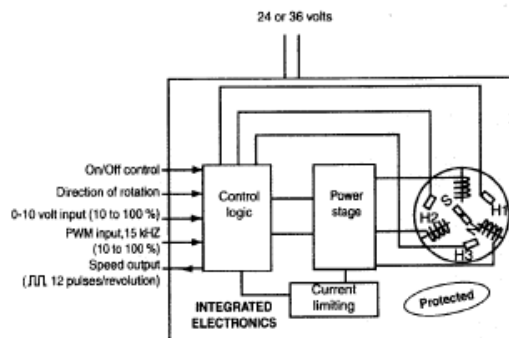
The voltage V is not significant (between 5 and 28 V), and does not affect the speed.

The PWM input is a digital input : it can be used by PLCs and micro-controllers.

■ Motor protection :

The motors are completely protected during operation : by current limiting and thermal protection. During abnormal operation, in a machine or device : for example locking, the motor stops after approximately 3 seconds, (power stage off) and must be reinitialised via the On/Off input : **this is a failsafe system.**

■ Inputs / Outputs :



■ Truth table for Inputs / Outputs :

On/Off	PWM	0-10 V	Direction	
0	x	x	x	motors off
1	1	0	0	reverse rotation
1	0	1	0	reverse rotation
1	1	1	0	unauthorised configuration
1	0	0	x	motors stopped
1	1	0	1	clockwise rotation
1	0	1	1	clockwise rotation
1	1	1	1	unauthorised configuration

X= don't care

1=Vih

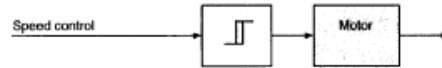
0=Vil

■ Speed regulation :

Two types of product with integrated electronics are offered for the whole range, both motors and geared motors.

a) No speed regulation : this option is offered for users who do not need to regulate speed in a closed loop, or who wish to reuse their own regulation electronics on an external card, to limit modifications to the architecture of their machine.

Motors without integrated speed regulation : no data feedback on action taken.

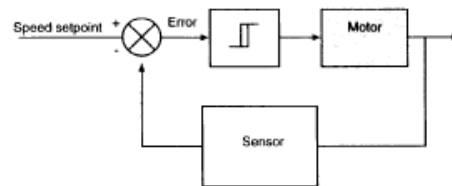


b) With integrated speed regulation (eg : Part no. 80 030 003) see page 10.

This integrated option can be used simply for a speed regulation function suitable for most applications. In effect : there is no longer any need to wire a motor to a card, no electromagnetic compatibility problems linked to wiring, hence reduced net cost!

Motor with integrated speed loop :

Hall effect sensors monitor the action taken, enabling the electronics to modify the command to achieve the desired effect.



4- Safety

Crouzet BRUSHLESS DC motors are designed and manufactured to be integrated into devices or machines which meet, for example, the specifications of the machine standard : EN 60335-1 (IEC 335-1, "Safety of domestic electrical appliances").

The integration of Crouzet DC motors into devices or machines, should generally take account of the following motor characteristics :

- no earth connection
- "main isolation" motors (simple isolation)
- protection index : IP40
- isolation system class : B (120°C)

European low voltage directive 73/23/EEC of 19/02/73 :

CROUZET DC motors and geared motors are outside the field of application of this directive (LVD 73/23/EEC applies to voltages over 75 volts DC).



5 - Electromagnetic Compatibility (EMC) :

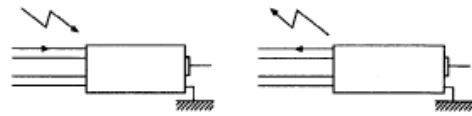
On request, Crouzet will provide the EMC characteristics of the various types of product.

European directive 89/336/EEC of 03/05/89, "electromagnetic compatibility" :

DC motors and geared motors which are components designed for professionals, to be incorporated in more complex devices, and not for end users, are excluded from the field of application of this directive.

However, conscious of potential customer difficulties concerning problems linked to electromagnetic compatibility, Crouzet has designed its products to meet the requirements of the standards : for example EN 55011 Gr. 1 class B (medical) as well as EN 55022, class B (data processing) in terms of emitted electromagnetic interference, as well as standards linked to immunity : IEC 1000- 4 -2/3/4/5/6/8.

■ Wiring precautions



- For EMC conformity :
- The motor must be connected to earth via its front flange.
 - The length of the wires is 20 cm.

6- Electrical characteristics

	Symbol	Conditions Ta = -10 to 40 °C	Min.	Nominal	Max.	Units
Active supply						
Supply voltage	Vmot	Version 1	10.8	24	28	V
		Version 2	32.4	36	39.6	V
Logic supply, ON/OFF INPUT						
Logic level 1	Vih		3		Vmot	V
Logic level 0	Vil		-1		1.7	V
Current for logic level 1	Iih				0.5	mA
Current for logic level 0	Iil				0.05	mA
5V Input						
Voltage	Vma		-1		Vmot	V
Input impedance	Ze			10		kΩ
5V Input with motor						
Logic level 1	Vih		3		28	V
Logic level 0	Vil		-1		1.7	V
Current for logic level 1	Iih				0.5	mA
Current for logic level 0	Iil				0.05	mA
PWM input frequency	Fin		13	15	17	kHz
Current limiting						
Voltage for level 0	Vol	Vih = 5 V, R pull up = 1.2 kΩ			0.4	V
Voltage for level 1	Voh				35	V
Current for level 0	Iol				5	mA
Current for level 1	Ioh				0.8	mA
Width of low level	Wle			320		µs
Current limiting						
Limit value	I _{max}	Ta = 20 °C, electronics at ambient 20 °C			3	A
Derating	I _{dt}			-23		mA/°C

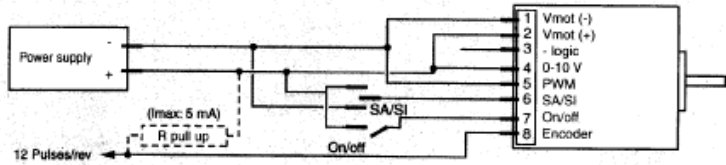
7 - Connection diagrams

General precautions : see page 7, 8, 10.
Connector marking : see page 10.

■ Simplified connection

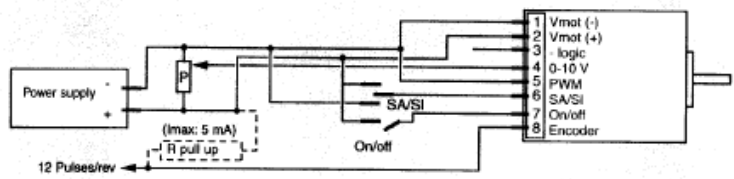
This connection only requires a power supply (24 or 36 V, 3 A).
Point 3 should not be connected.

This diagram can be further simplified by connecting input 7 directly to the power supply positive and input 6 either to the power supply positive or negative depending on the direction of rotation required.



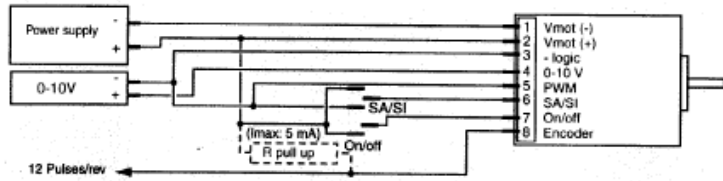
■ Adjusting the speed using a potentiometer

Point 3 should not be connected.



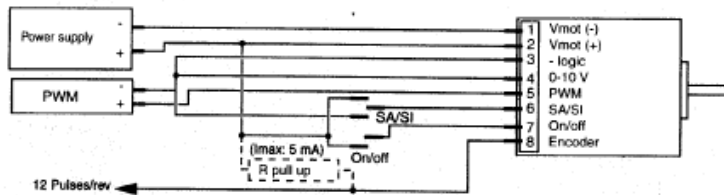
■ Using the 0-10 V input, with a separate power supply

This connection requires a power supply (24 or 36 V, 3 A) and a 0-10 V supply.



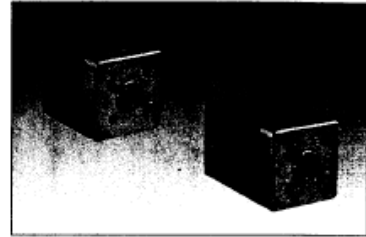
■ Using the PWM input

This connection requires a power supply (24 or 36 V, 3 A) and a supply with PWM and a frequency of 15 kHz.



BRUSHLESS DC motors

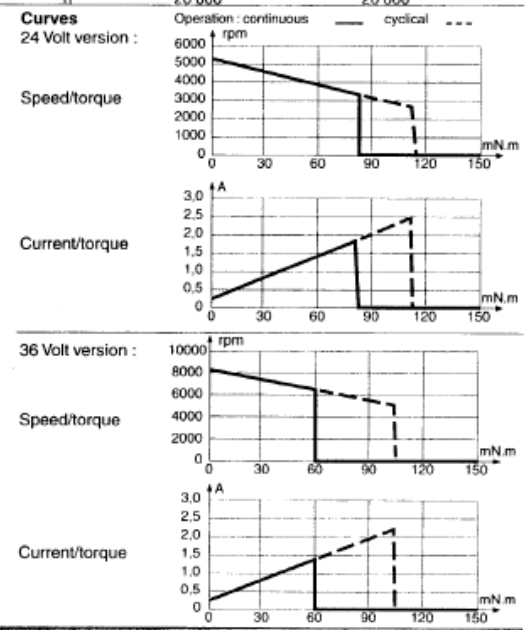
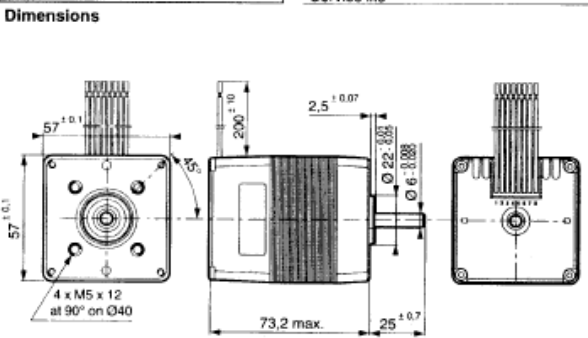
- Brushless motors with integrated speed regulation without integrated speed regulation
- Maximum power : 35 to 60 W
- Long service life
- Motors with integrated temperature sensor
- Conform to EMC standards
- Emissions EN 55022 / EN 55024



- ### Applications
- Pumps, turbines
 - Compressors
 - Gas analysers
 - Dialysis equipment
 - Physiotherapy equipment
 - Respirators
 - Copiers and peripherals
 - Postal sorting systems
 - Bank processing systems
 - Motor-driven fans
 - Engraving machines
 - Textiles
 - Packaging
 - Automated materials handling belts
 - Aerials and radar

Type	80 030	80 030	
Nominal voltages	24 V	36 V	
Part numbers			
Without speed regulation	80 030 002	80 030 004	
With speed regulation	80 030 003	80 030 005	
No-load characteristics			
Speed of rotation	rpm	5400	8300
Absorbed power	W	5	8
Absorbed current	A	0.22	0.23
Nominal characteristics (acc. to IEC 68-2-14) given for 100% of nominal speed			
Speed of rotation (adjustable from 10 to 100%)	rpm	3410	6500
Torque	mN.m	85	60
Usable power	W	30	42
Absorbed power	W	45	58
Casing temperature	°C	62	62
Ambient temperature	°C	-10 to +40	-10 to +40
Efficiency	%	66	72
General characteristics			
Precision of speed regulation	%	± 5	± 5
Isolation system acc. to IEC 85		B (120 °C)	B (120 °C)
Degree of protection acc. to IEC 529		IP40	IP40
Maximum usable power	W	35	60
Starting torque	mN.m	115	100
Starting current	A	2.5	2.2
Maximum efficiency	%	75	75
Acoustic pressure (at 50 cm)	dBA	40	44
Resistance	Ω	2.1	2.1
Inductance	mH	4	4
Torque constant	Nm/A	0.045	0.04
Electrical time constant	ms	1.9	1.9
Mechanical time constant	ms		
Thermal time constant	min	5	5
Thermal impedance winding/ambient air	°C/W	2.2	2.2
Inertia	g.cm ²	28	28
Weight	g	800	800
Service life	h	20 000	20 000

- ### OPTIONS : on request
- Integrated speed regulation
 - High-resolution encoder from 100 to 512 pulses/rev
 - Adaptations with front/rear shaft in stainless steel
 - Motors with Hall sensors only
 - Adaptations on electronics
 - Alternative protection index : IP54



Connections

AMP MTA 100 640440-8 connector with AWG22 wire, Ø on insulation 1.8 mm (supplied)

Marking on motor	Wire colour	
1	* a	Black 0 volt reference for the power supply
2	* a	Red Power supply (24 or 36 V)
3	* b	Blue 0 volt reference for control (not isolated from 1)
4		Brown 0-10 volt speed analogue input
5		Orange PWM speed digital input (15 KHz)
6	* c	Yellow Logic input, direction of rotation (1-clockwise direction)
7		Green Logic input, run/stop (1=run)
8		White Encoder logic output, 12 pulses per revolution

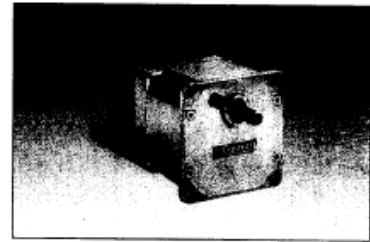
Necessary precautions to avoid damaging the motor
 *a) Do not reverse the polarity. *b) If only 1 power supply is being used, do not connect 3 to 1.
 *c) Stop the motor before changing direction.

To order specify

Standard products **1** Part number
 Example : BRUSHLESS DC motor - 80 030 002



BRUSHLESS DC geared motors



- Special reduction ratio
- Special greasing
- Shaft adaptation
- Stainless steel shaft option
- Motor : see page 10

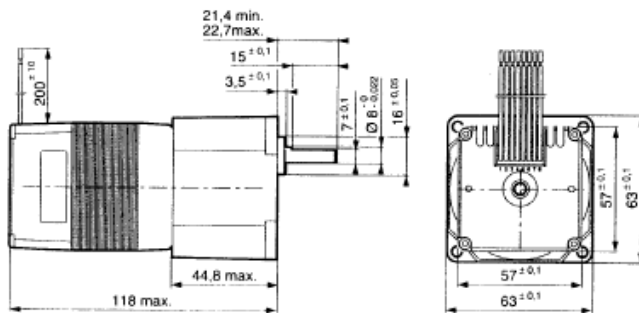
Types

		80 035 5	80 035 5
Nominal voltage		24 V	24 V
Gearbox output speeds (rpm)		Part numbers	
Without speed regulation		•	
With speed regulation		•	
10%	100% of speed (rpm)	Ratios	
81 to 806		4.22	80 035 501
51 to 504		6.75	80 035 508
45 to 444		7.66	80 035 502
28 to 278		12.25	80 035 509
23 to 222		15.31	80 035 503
14 to 139		24.5	80 035 510
9 to 89		38.28	80 035 511
7 to 69		49	80 035 505
6 to 56		61.25	80 035 512
3 to 28		122.5	
1.5 to 14		245	

General characteristics

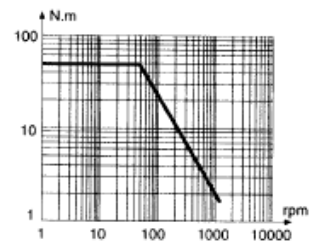
Motor		80 030	80 030
Gearbox		81 035 5	81 035 5
Maximum permitted gearbox torque in steady state	Nm	5	5
Axial load (dynamic)	daN	6	6
Radial load (dynamic)	daN	6	6
Nominal usable power	W	24	24
Casing temperature	°C	58	58
Weight	g	1300	1300

Dimensions



Curve : nominal torque/speed

The unbroken line represents the maximum operating ranges for the geared motors in continuous operation.



Standard products

3 Part number
Example : Brushless DC geared motor - 80 035 502

1 Type **2** Nominal voltage **3** Output speed
Example : BRUSHLESS DC geared motor - 80 035 5 - 24 V - With speed regulation 222 rpm.



Low-Cost Multifunction DAQ for USB

NI USB-6008, NI USB-6009

- Small and portable
- 12 or 14-bit input resolution, at up to 48 kS/s
- Built-in, removable connectors for easier and more cost-effective connectivity
- 2 true DAC analog outputs for accurate output signals
- 12 digital I/O lines (TTL/LVTTL/CMOS)
- 32-bit event counter
- Student kits available
- OEM versions available

Operating Systems

- Windows 2000/XP
- Mac OS X¹
- Linux[®]1
- Pocket PC
- Win CE

Recommended Software

- LabVIEW
- LabWindows/CVI

Measurement Services Software (included)

- NI-DAQmx
- Ready-to-run data logger

¹Mac OS X and Linux users need to download NI-DAQmx Base.



Product	Bus	Analog Inputs ¹	Input Resolution (bits)	Max Sampling Rate (kS/s)	Input Range (V)	Analog Outputs	Output Resolution (bits)	Output Rate (Hz)	Output Range (V)	Digital I/O Lines	32-Bit Counter	Trigger
USB-6009	USB	8 SE/A DI	14	48	±1 to ±20	2	12	150	0 to 5	12	1	Digital
USB-6008	USB	8 SE/A DI	12	10	±1 to ±20	2	12	150	0 to 5	12	1	Digital

¹SE = single ended, DI = differential

Hardware Description

The National Instruments USB-6008 and USB-6009 multifunction data acquisition (DAQ) modules provide reliable data acquisition at a low price. With plug-and-play USB connectivity, these modules are simple enough for quick measurements but versatile enough for more complex measurement applications.

Software Description

The NI USB-6008 and USB-6009 use NI-DAQmx high-performance, multithreaded driver software for interactive configuration and data acquisition on Windows OSs. All NI data acquisition devices shipped with NI-DAQmx also include VI Logger Lite, a configuration-based data-logging software package.

Mac OS X and Linux users can download NI-DAQmx Base, a multiplatform driver with a limited NI-DAQmx programming interface. You can use NI-DAQmx Base to develop customized data acquisition applications with National Instruments LabVIEW or C-based development environments. NI-DAQmx Base includes a ready-to-run data logger application that acquires and logs up to eight channels of analog data.

PDA users can download NI-DAQmx Base for Pocket PC and Win CE to develop customized handheld data acquisition applications.

Recommended Accessories

The USB-6008 and USB-6009 have removable screw terminals for easy signal connectivity. For extra flexibility when handling multiple wiring configurations, NI offers the USB-6008/09 Accessory Kit, which includes two extra sets of screw terminals, extra labels, and a screwdriver.

In addition, the USB-6008/09 Prototyping Accessory provides space for adding more circuitry to the inputs of the USB-6008 or USB-6009.

Common Applications

The USB-6008 and USB-6009 are ideal for a number of applications where economy, small size, and simplicity are essential, such as:

- Data logging – Log environmental or voltage data quickly and easily.
- Academic lab use – The low price facilitates student ownership of DAQ hardware for completely interactive lab-based courses. (Academic pricing available. Visit ni.com/academic for details.)
- Embedded OEM applications.



Low-Cost Multifunction DAQ for USB

Information for Student Ownership

To supplement simulation, measurement, and automation theory courses with practical experiments, NI has developed the USB-6008 and USB-6009 student kits, which include the LabVIEW Student Edition and a ready-to-run data logger application. These kits are exclusively for students, giving them a powerful, low-cost hands-on learning tool. Visit ni.com/academic for more details.

Information for OEM Customers

For information on special configurations and pricing, call (800) 813 3693 (U.S. only) or visit ni.com/oem. Go to the Ordering Information section for part numbers.

Ordering Information

NI USB-6008 ¹	779051-01
NI USB-6009 ¹	779026-01
NI USB-6008 OEM	193132-02
NI USB-6009 OEM	193132-01
NI USB-6008 Student Kit ^{1,2}	779320-22
NI USB-6009 Student Kit ^{1,2}	779321-22

¹Includes NI-DAQmx software, NI ready-to-run data logger software, and a USB cable.

²Includes LabVIEW Student Edition.

BUY NOW!

For complete product specifications, pricing, and accessory information, call 800 265 9891 (U.S. only) or go to ni.com/usb.

BUY ONLINE at ni.com or **CALL** (800) 813 3693 (U.S.)

Low-Cost Multifunction DAQ for USB

Specifications

Typical at 25 °C unless otherwise noted.

Analog Input

Absolute accuracy, single-ended

Range	Typical at 25 °C (mV)	Maximum (0 to 55 °C) (mV)
±10	14.7	138

Absolute accuracy at full scale, differential¹

Range	Typical at 25 °C (mV)	Maximum (0 to 55 °C) (mV)
±20	14.7	138
±10	7.73	84.8
±5	4.28	58.4
±4	3.58	53.1
±2.5	2.56	45.1
±2	2.21	42.5
±1.25	1.70	38.9
±1	1.53	37.5

Number of channels..... 8 single-ended/4 differential
 Type of ADC Successive approximation

ADC resolution (bits)

Module	Differential	Single-Ended
USB-6008	12	11
USB-6009	14	13

Maximum sampling rate (system dependent)

Module	Maximum Sampling Rate (kS/s)
USB-6008	10
USB-6009	48

Input range, single-ended..... ±10 V
 Input range, differential..... ±20, ±10, ±5, ±4, ±2.5, ±2, ±1.25, ±1 V
 Maximum working voltage ±10 V
 Overvoltage protection ±35 V
 FIFO buffer size 512 B
 Timing resolution 41.67 ns (24 MHz timebase)
 Timing accuracy 100 ppm of actual sample rate
 Input impedance 144 k
 Trigger source..... Software or external digital trigger
 System noise..... 0.3 LSB_{rms} (±10 V range)

Analog Output

Absolute accuracy (no load) 7 mV typical, 36.4 mV maximum at full scale
 Number of channels..... 2
 Type of DAC Successive approximation
 DAC resolution 12 bits
 Maximum update rate 150 Hz, software-timed

¹Input voltages may not exceed the working voltage range.

Output range 0 to +5 V
 Output impedance..... 50 Ω
 Output current drive 5 mA
 Power-on state 0 V
 Slew rate..... 1 V/μs
 Short-circuit current..... 50 mA

Digital I/O

Number of channels..... 12 total
 8 (P0.<0..7>)
 4 (P1.<0..3>)
 Direction control Each channel individually programmable as input or output
 Output driver type
 USB-6008 Open-drain
 USB-6009 Each channel individually programmable as push-pull or open-drain
 Compatibility CMOS, TTL, LVTTL
 Internal pull-up resistor 4.7 kΩ to +5 V
 Power-on state Input (high impedance)
 Absolute maximum voltage range..... -0.5 to +5.8 V

Digital logic levels

Level	Min	Max	Units
Input low voltage	-0.3	0.8	V
Input high voltage	2.0	5.8	V
Input leakage current	–	50	μA
Output low voltage (I = 8.5 mA)	–	0.8	V
Output high voltage (push-pull, I = -8.5 mA)	2.0	3.5	V
Output high voltage (open-drain, I = -0.6 mA, nominal)	2.0	5.0	V
Output high voltage (open-drain, I = -8.5 mA, with external pull-up resistor)	2.0	–	V

Counter

Number of counters 1
 Resolution 32 bits
 Counter measurements..... Edge counting (falling edge)
 Pull-up resistor..... 4.7 kΩ to 5 V
 Maximum input frequency 5 MHz
 Minimum high pulse width..... 100 ns
 Minimum low pulse width 100 ns
 Input high voltage 2.0 V
 Input low voltage 0.8 V

Power available at I/O connector

+5 V output (200 mA maximum) +5 V typical
 +4.85 V minimum
 +2.5 V output (1 mA maximum) +2.5 V typical
 +2.5 V output accuracy 0.25% max
 Voltage reference temperature drift... 50 ppm/°C max

BUY ONLINE at ni.com or CALL (800) 813 3693 (U.S.)

Low-Cost Multifunction DAQ for USB

Physical Characteristics

If you need to clean the module, wipe it with a dry towel.

Dimensions (without connectors)	6.35 by 8.51 by 2.31 cm (2.50 by 3.35 by 0.91 in.)
Dimensions (with connectors)	8.18 by 8.51 by 2.31 cm (3.22 by 3.35 by 0.91 in.)
Weight (without connectors)	59 g (2.1 oz)
Weight (with connectors)	84 g (3 oz)
I/O connectors	USB series B receptacle (2) 16-position (screw-terminal) plug headers
Screw-terminal wiring	16 to 28 AWG
Screw-terminal torque	0.22 to 0.25 N•m (2.0 to 2.2 lb•in.)

Power Requirement

USB (4.10 to 5.25 VDC)	80 mA typical 500 mA maximum
USB suspend	300 μ A typical 500 μ A maximum

Environmental

The USB-6008 and USB-6009 are intended for indoor use only.

Operating environment	
Ambient temperature range	0 to 55 °C (tested in accordance with IEC-60068-2-1 and IEC-60068-2-2)
Relative humidity range	10 to 90%, noncondensing (tested in accordance with IEC-60068-2-56)
Storage environment	
Ambient temperature range	-40 to 85 °C (tested in accordance with IEC-60068-2-1 and IEC-60068-2-2)
Relative humidity range	5 to 90%, noncondensing (tested in accordance with IEC-60068-2-56)
Maximum altitude	2,000 m (at 25 °C ambient temperature)
Pollution degree	2

Safety and Compliance

Safety

This product is designed to meet the requirements of the following standards of safety for electrical equipment for measurement, control, and laboratory use:

- IEC 61010-1, EN 61010-1
- UL 61010-1, CAN/CSA-C22.2 No. 61010-1

Note: For UL and other safety certifications, refer to the product label or visit ni.com/certification, search by model number or product line, and click the appropriate link in the Certification column.

Electromagnetic Compatibility

This product is designed to meet the requirements of the following standards of EMC for electrical equipment for measurement, control, and laboratory use:

- EN 61326 EMC requirements; Minimum Immunity
- EN 55011 Emissions; Group 1, Class A
- CE, C-Tick, ICES, and FCC Part 15 Emissions; Class A

Note: For EMC compliance, operate this device according to product documentation.

CE Compliance

This product meets the essential requirements of applicable European Directives, as amended for CE marking, as follows:

- 73/23/EEC; Low-Voltage Directive (safety)
- 89/336/EEC; Electromagnetic Compatibility Directive (EMC)

Note: Refer to the Declaration of Conformity (DoC) for this product for any additional regulatory compliance information. To obtain the DoC for this product, visit ni.com/certification, search by model number or product line, and click the appropriate link in the Certification column.

Waste Electrical and Electronic Equipment (WEEE)

EU Customers: At the end of their life cycle, all products must be sent to a WEEE recycling center. For more information about WEEE recycling centers and National Instruments WEEE initiatives, visit ni.com/environment/weee.htm.

BUY ONLINE at ni.com or CALL (800) 813 3693 (U.S.)

NI Services and Support



NI has the services and support to meet your needs around the globe and through the application life cycle – from planning and development through deployment and ongoing maintenance. We offer services and service levels to meet customer requirements in research, design, validation, and manufacturing. Visit ni.com/services.

Training and Certification

NI training is the fastest, most certain route to productivity with our products. NI training can shorten your learning curve, save development time, and reduce maintenance costs over the application life cycle. We schedule instructor-led courses in cities worldwide, or we can hold a course at your facility. We also offer a professional certification program that identifies individuals who have high levels of skill and knowledge on using NI products. Visit ni.com/training.

Professional Services

Our Professional Services Team is comprised of NI applications engineers, NI Consulting Services, and a worldwide National Instruments Alliance Partner program of more than 600 independent consultants and



integrators. Services range from start-up assistance to turnkey system integration. Visit ni.com/alliance.

OEM Support

We offer design-in consulting and product integration assistance if you want to use our products for OEM applications. For information about special pricing and services for OEM customers, visit ni.com/oem.

Local Sales and Technical Support

In offices worldwide, our staff is local to the country, giving you access to engineers who speak your language. NI delivers industry-leading technical support through online knowledge bases, our applications engineers, and access to 14,000 measurement and automation professionals within NI Developer Exchange forums. Find immediate answers to your questions at ni.com/support.

We also offer service programs that provide automatic upgrades to your application development environment and higher levels of technical support. Visit ni.com/ssp.

Hardware Services

NI Factory Installation Services

NI Factory Installation Services (FIS) is the fastest and easiest way to use your PXI or PXI/SCXI combination systems right out of the box. Trained NI technicians install the software and hardware and configure the system to your specifications. NI extends the standard warranty by one year on hardware components (controllers, chassis, modules) purchased with FIS. To use FIS, simply configure your system online with ni.com/pxiadvisor.

Calibration Services

NI recognizes the need to maintain properly calibrated devices for high-accuracy measurements. We provide manual calibration procedures, services to recalibrate your products, and automated calibration software specifically designed for use by metrology laboratories. Visit ni.com/calibration.

Repair and Extended Warranty

NI provides complete repair services for our products. Express repair and advance replacement services are also available. We offer extended warranties to help you meet project life-cycle requirements. Visit ni.com/services.



ni.com • (800) 813 3693

National Instruments • info@ni.com



351378A-01

2006-7322-301-101-0

© 2006 National Instruments Corporation. All rights reserved. CVI, LabVIEW, National Instruments, National Instruments Alliance Partner, NI, ni.com, and SCXI are trademarks of National Instruments. Linux® is a registered trademark of Linus Torvalds in the U.S. and other countries. Other product and company names listed are trademarks or trade names of their respective companies. A National Instruments Alliance Partner is a business entity independent from NI and has no agency, partnership, or joint-venture relationship with NI.